Journal of Microscopy, Vol. 221, Pt 2 February 2006, pp. 89–109
Received 28 July 2005; accepted 20 October 2005

The quantitative analysis of thin specimens: a review of progress from the Cliff-Lorimer to the new ζ-factor methods

M. WATANABE & D. B. WILLIAMS
Department of Materials Science and Engineering/Center for Advanced Materials and Nanotechnology, Lehigh University, Bethlehem, PA 18015, U.S.A.

Key words. Absorption correction, Cliff-Lorimer ratio technique, detector efficiency, light-element analysis, minimum detectable mass, minimum mass fraction, pure-element thin-film standard, quantitative thin-film X-ray analysis, spatial resolution, thickness determination, ζ (zeta)-factor method.

Summary

A new quantitative thin-film X-ray analysis procedure termed the ζ-factor method is proposed. This new ζ-factor method overcomes the two major limitations of the conventional Cliff-Lorimer method for quantification: (1) use of pure-element rather than multielement, thin-specimen standards and (2) built-in X-ray absorption correction with simultaneous thickness determination. Combined with a universal, standard, thin specimen, a series of ζ-factors covering a significant fraction of the periodic table can be estimated. This ζ-factor estimation can also provide information about both the detector efficiency and the microscope–detector interface system. Light-element analysis can also be performed more easily because of the built-in absorption correction. Additionally, the new ζ-factor method has several advantages over the Cliff-Lorimer ratio method because information on the specimen thickness at the individual analysis points is produced simultaneously with compositions, thus permitting concurrent determination of the spatial resolution and the analytical sensitivity. In this work, details of the ζ-factor method and how it improves on the Cliff-Lorimer approach are demonstrated, along with several applications.

Introduction

It is 30 years since the Cliff-Lorimer ratio technique (Cliff & Lorimer, 1975) was first introduced as a method for quantitative thin-film microanalysis using X-ray energy dispersive spectrometry (XEDS) in analytical electron microscopes (AEMs). The ratio approach was originally taken to overcome the design limitations of the early AEMs, namely the very low X-ray generation and detection rates, electrical and mechanical instabilities (particularly the beam current) and the tendency to contaminate the analysis area, all of which meant that the X-ray count rates were invariably poor, thus limiting quantification. These limitations meant that it was not feasible to use the well-established, pure-element standards approach developed over the preceding 25 years for bulk analysis in the electron probe microanalyser (EPMA). A ratio approach removes much of the instrument variability as it cancels out any variations in the probe current incident on the analysis area, which arise from electron-gun/condenser-system instabilities, drift and contamination build-up. Despite the fact that many of these instrument limitations have been minimized in the intervening three decades, the ratio technique still remains the only quantitative thin-film analysis software available on commercial XEDS systems. Clearly this is not an ideal situation and this work first reviews the limitations of the Cliff-Lorimer method and then proposes an alternative, improved approach, which combines the ease of application of the ratio method with the more rigorous aspects of pure-element (or other) thin-film standards.

In order to stress the advantages of the ζ-factor method, it is worthwhile reviewing the Cliff-Lorimer approach, which relates the compositions of the constituent elements C_A and C_B (usually, but not necessarily, defined as the weight fraction or wt%) in a thin specimen to the measured characteristic X-ray intensities above background (I_A and I_B) as

$$\frac{C_A}{C_B} = k_{AB}\frac{I_A}{I_B} \qquad (1)$$

where k_{AB} is the Cliff-Lorimer factor, which can be determined both theoretically and experimentally (e.g. Goldstein *et al.*, 1977; Williams & Carter, 1996). Obviously, determination of the *k*-factor is the critical step for consequent quantification. The theoretical calculation of *k*-factors from first principles is fast and easy but may produce significant (±15–20% relative) systematic errors (e.g. Maher *et al.*, 1981; Newbury *et al.*, 1984).

Correspondence to: Dr Masashi Watanabe. Fax: +1(610)758-3526; e-mail: masashi.watanabe@lehigh.edu

On the other hand, *k*-factors can be determined experimentally with relative errors of as little as approx. ±1% (e.g. Wood *et al.*, 1984; Sheridan, 1989) and hence more accurate quantification can be performed in many cases using the experimental *k*-factors. To determine the *k*-factors experimentally, multiple, standard thin-films with known composition are required. Unfortunately, this requirement is not always an option for the analyst because such standards may not be available and, even if all the requisite standards are available, many *k*-factors still need to be determined in a multicomponent system. Furthermore, the standards may be difficult to thin to electron transparency and may be susceptible to damage (including compositional changes) during thinning and subsequent high-energy electron bombardment in the AEM. Thus, experimental *k*-factor determination can be extremely tedious and time consuming, which accounts for the relatively few examples of experimental suites of *k*-factors described in the literature over the last 30 years and the consequent tendency of most analytical microscopists to use the quick (and often inaccurate) theoretical calculations.

In addition to these limitations, there are other problems with the Cliff-Lorimer method. One of the most serious problems is X-ray absorption, even in thin specimens. Goldstein *et al.* (1977) derived a formula to correct for X-ray absorption in thin specimens with finite thickness by multiplying Eq. (1) with an absorption-correction term. Unfortunately, in order to apply the X-ray absorption correction, prior knowledge of the specimen thickness and density is required at the individual analysis points. As independent measurements are usually required for the specimen density and thickness, inaccuracies associated with such measurements may cause further errors in quantification. Obviously, the need for an absorption correction is a major limitation to the accurate quantitative microanalysis of thin specimens.

This work describes a new quantitative thin-film analysis procedure, which builds on a previously published approach (Watanabe *et al.*, 1996; Watanabe & Williams, 1999a, 2003) termed the ζ-factor method. Unlike the earlier versions, this new ζ-factor method overcomes all the above limitations in the Cliff-Lorimer method. Detailed methods for the ζ-factor determination using pure element (PE) standards [as well as National Institute of Standards and Technology (NIST) standard thin specimens] will be given and statistical error treatments in both the ζ-factor determination and the quantification will then be discussed. Additionally, several advantages of the ζ-factor method over the Cliff-Lorimer ratio method mainly due to the '*in-situ*' thickness determination from the built-in absorption correction will be described, e.g. light-element analysis, calculation of the spatial resolution and determination of the analytical sensitivities. If the NIST standard thin specimen is used for the ζ-factor estimation, the XEDS detector efficiency can also be evaluated. A ζ-factor for a hard X-ray line such as the Fe Kα can also be used as a figure of merit to evaluate the system performance of an AEM–XEDS interface. Finally, the limitations of the ζ-factor method will also be addressed.

Theory of the ζ-factor method

Definition of the ζ-factor

In a thin-film specimen, it can be assumed that the measured characteristic X-ray intensity (which is the number of X-ray photons above background, integrated over a certain energy range) is proportional to the mass-thickness ρt (ρ and t are the specimen density and thickness, respectively) and the composition C_A. Therefore, the mass-thickness can be related to the measured X-ray intensity I_A normalized by the composition, if absorption and fluorescence of X-ray are negligible (i.e. the thin-film approximation)

$$\rho t = \zeta_A \frac{I_A}{C_A D_e} \tag{2}$$

where ζ_A is a proportional factor connecting I_A to ρt and C_A, and D_e is the total electron dose during acquisition, defined as

$$D_e = N_e I_p \tau \tag{3}$$

N_e is the number of electrons (electron counts) in a unit electric charge and I_p and τ are the beam current and acquisition time, respectively. It should be noted that the above Eq. (2) is modified from the originally proposed expression (Watanabe *et al.*, 1996; Watanabe & Williams, 1999a, 2003) by incorporating the electron-dose term D_e. Thus, the new ζ-factor is no longer dependent on the acquisition time or the beam current, in addition to its original independence from the composition and mass-thickness. This modification is practically very useful because the new ζ-factor does not need to be adjusted for individual experimental conditions with different beam currents or different acquisition times, which change depending on specific analysis needs. Accordingly, the units for the new ζ-factor are modified to kg·electron/(m^2·photon) instead of kg/(m^2·photon).

The measured X-ray intensity from element A can theoretically be described by the following equation in the thin-film approximation (e.g. Armigliato, 1992)

$$I_A = N_v \frac{Q_A \omega_A a_A}{M_A} C_A \rho t D_e \left(\frac{\Omega}{4\pi}\right) \varepsilon_A \tag{4}$$

where N_v is Avogadro's number, Q_A is the ionization cross-section, ω_A is the fluorescence yield, a_A is the relative transition probability (i.e. the relative line weight), M_A is the atomic weight, $\Omega/(4\pi)$ is the detector collection-angle in the whole 4π space and ε_A is the detector efficiency. By comparison with Eq. (2), the theoretical expression for the new ζ-factor is

$$\zeta_A = \frac{M_A}{N_v Q_A \omega_A a_A [\Omega/(4\pi)] \varepsilon_A} \tag{5}$$

All the parameters associated with X-ray generation in a thin specimen and X-ray detection in an AEM are thus incorporated

into the new ζ-factor. In other words, the new ζ-factor is dependent only on the X-ray energy and the accelerating voltage and is independent of the total electron dose, specimen composition, thickness and density. As shown below, this independence makes any absorption correction trivial, a significant step forward from the Cliff-Lorimer approach.

Quantification via ζ-factors

The original ζ-factor method was based on the X-ray absorption correction in the Cliff-Lorimer ratio method (Watanabe *et al*., 1996). Applying this technique to quantitative thin-specimen analyses in AEM removed the need for independent thickness determinations. The absorption-corrected compositions could be determined simultaneously with the specimen thickness at the individual measured points. However, there are still major limitations: (1) the requirement that at least one characteristic X-ray line in the spectrum was free of any significant absorption correction (needed to monitor the specimen thickness) and (2) the approach was still based on the Cliff-Lorimer ratio equation, so *k*-factors were still required (and hence all the issues associated with *k*-factor determination mentioned above also remained).

The ζ-factor method was recently modified to overcome the above limitations (Watanabe & Williams, 1999a, 2003). A similar relationship to Eq. (2) can be established between ρt and I_B using the ζ-factor for element B, ζ_B

$$\rho t = \zeta_B \frac{I_B}{C_B D_e} \tag{6}$$

From Eqs (2) and (6), C_A, C_B, and ρt can be expressed assuming $C_A + C_B = 1$ in a binary system

$$\rho t = \frac{\zeta_A I_A + \zeta_B I_B}{D_e}, \quad C_A = \frac{\zeta_A I_A}{\zeta_A I_A + \zeta_B I_B}, \quad C_B = \frac{\zeta_B I_B}{\zeta_A I_A + \zeta_B I_B} \tag{7}$$

Therefore, C_A, C_B, and ρt can be determined simultaneously from measured X-ray intensities but *k*-factors are no longer required. This approach can be easily expanded to any multicomponent systems as long as $\Sigma C_j = 1$, which is a reasonable assumption. It should be noted that the resultant compositions and thickness could be over- and/or underestimated by the ζ-factor method if any major components in the system were missed in quantification. Therefore, all the major components must be quantified and qualitative analysis should be performed prior to quantification (Williams & Carter, 1996). In the ζ-factor method, the *in-situ* beam-current measurement during the analysis is the most crucial.

The absolute specimen thickness t can also be obtained if the specimen density is known at the analysis point. The specimen density can be estimated from the crystallographic unit-cell information. Otherwise, the density can be calculated as a first approximation by taking a weighted mean ($\rho = \Sigma C_j \rho_j$) or a harmonic mean ($1/\rho = \Sigma C_i/\rho_j$) from the density values of the individual component elements. These density estimations, especially the harmonic-mean approach, may work well for the close-packed condensed systems, such as metallic alloys and intermetallic compounds.

Integration of correction terms for X-ray intensity

One of the most serious problems in quantitative X-ray analysis, even in thin specimens, is X-ray absorption. Goldstein *et al*. (1977) derived a formula to correct the Cliff-Lorimer ratio equation [Eq. (1)] for X-ray absorption. However, in order to apply this X-ray absorption correction, prior knowledge of the specimen thickness and density was required at all individual measured points. As independent measurements are usually required for the determination of the specimen density and thickness, inaccuracies associated with such measurements may cause further errors in quantification. This requirement is the major difficulty in using the absorption correction and limits the accuracy of quantitative X-ray analysis of thin specimens in AEMs.

Several methods have been proposed to avoid the difficulties and complications arising from the need for thickness and density determinations. These approaches can be categorized broadly into two types: (1) the extrapolation method, which determines the absorption correction by extrapolation of X-ray intensity ratios to zero thickness (e.g. Porter & Westengen, 1981; Horita *et al*., 1987; Van Cappellen, 1990; Eibl, 1993) and (2) utilization of the difference in relative X-ray absorption between two emitted X-ray lines (K and L, or L and M) from the same element, described as the K : L intensity-ratio method or the differential X-ray absorption method (e.g. Morris *et al*., 1980; Horita *et al*., 1989). Unfortunately, these two techniques are also limited. The extrapolation method is not easily applicable to thin-foils where compositions vary locally, as a series of X-ray intensities has to be obtained from different thickness areas (by moving the incident beam or by tilting the specimen). In addition, if a series of X-ray intensities is measured from the same position at multiple tilts rather than a single tilt, the X-ray absorption can also be corrected. This approach, called the multigeometry method, can eliminate the determination of the specimen thickness, the density and measurement of the beam current (Statham & Ball, 1980). Note that when using the multigeometry method it was found that, when the thin foil is buckled or wedge-shaped, the exact geometry and absorption path length differ from that for a plane, parallel-sided foil. Ultimately, this approach requires that many X-ray intensity measurements must be made from one specific region, which still makes the X-ray absorption correction rather complicated and tedious. In the K : L intensity ratio method, the essential requirement of two different X-ray lines from a single element limits the application to specimens that contain elements with $Z > 20$ (Ca).

The X-ray absorption correction can be integrated into the ζ-factor method in the same way that Goldstein *et al*. (1977)

modified Eq. (1). The absorption-correction term for a single X-ray line from a thin specimen can be given as (Philibert, 1963)

$$A_A = \frac{(\mu/\rho)^A_{sp}\,\rho t\,\mathrm{cosec}\,\alpha}{1-\exp[-(\mu/\rho)^A_{sp}\,\rho t\,\mathrm{cosec}\,\alpha]} \quad (8)$$

where $(\mu/\rho)^A_{sp}$ is the mass absorption coefficients of the characteristic X-ray line in the specimen and α is the X-ray take-off angle. This absorption-correction term is incorporated into the ζ-factor by multiplying it by the corresponding X-ray intensities in Eq. (7). Therefore, the general expressions for the quantitative ζ-factor analysis can be modified as

$$\rho t = \sum_j^N \frac{\zeta_j I_j A_j}{D_e}, \quad C_A = \frac{\zeta_A I_A A_A}{\sum_j^N \zeta_j I_j A_j}, \quad \ldots, \quad C_N = \frac{\zeta_N I_N A_N}{\sum_j^N \zeta_j I_j A_j} \quad (9)$$

An iterative process is required to solve the above equations for the composition and thickness determination. However, the iteration in Eq. (9) is straightforward and the convergence rate is typically very fast (e.g. up to 10–15 iterations are typically required to converge to less than 0.001 wt% and 0.01-nm differences in the composition and the specimen thickness, respectively, which are more than sufficient tolerance values for the termination). A complete flow chart for the quantification procedure via the ζ-factor method is summarized in Fig. 1. If the X-ray absorption is negligible in a material system, the initial mass-thickness and compositions are the final values and the iteration is no longer necessary. In the ζ-factor method, the absorption-corrected compositions can be determined simultaneously with the specimen mass-thickness only from X-ray intensity data. It should be noted that a fluorescence correction can also be incorporated in a similar manner in the few situations where X-ray fluorescence is significant, such as an analysis of minor amounts of Cr in Fe (e.g. Nockolds *et al.*, 1980).

Determination of ζ-factors

Use of pure-element, thin-film standards

Quantitative X-ray analysis via the ζ-factors is as easy as the Cliff-Lorimer method, so long as the ζ-factors are already known. To determine the ζ-factors, X-ray intensities should be measured from standard, thin films with known composition and thickness, as shown in Eqs (2) and (6). As the ζ-factor consists of information from only a single element, PE thin films can be used as standards in addition to thin films of known composition. This option of using PE standard, thin films is a major experimental step forward because, compared with multielement standards for *k*-factors, PE films have the distinct advantages of being robust, cheap, easy to fabricate and insensitive to un-noticed specimen drift. Most importantly, they do not change composition during thinning to electron transparency or as a result of beam damage. By using modern thin-film fabrication techniques such as sputtering and electron deposition, the thickness of the PE films can be precisely controlled within a few Ångstroms. It is also possible to use other preparation techniques, such as evaporation, ultramicrotomy and focused ion-beam. If the PE thin specimens are prepared by these methods, the film thickness required for the ζ-factor determination can be measured relatively easily by profilometry, atomic-force microscopy, cross-section scanning electron microscopy and electron energy-loss spectrometry in AEMs. In addition to the above advantages, the X-ray absorption is negligible in most of the major characteristic lines generated from the PE thin films, which is clearly not the case for many multielement thin films [including the NIST standard reference materials (SRMs) 2063 and 2063a, which are discussed in detail later in this work]. The critical specimen thickness at which 5% of X-ray absorption occurs is plotted against the atomic number in Fig. 2. The shadowed area represents the thickness range < 30 nm, which may not be suitable as a standard for the ζ-factor method because generated X-ray intensities would not be sufficient in conventional AEMs. The critical thicknesses at 5% X-ray absorption are greater than 30 nm for all the K lines and most of the L lines that are higher than ~1 keV (above Zn). However, the critical thicknesses for most of the M lines are below 30 nm. The K lines above B and the L lines above Zn that are detectable in most AEMs cover most of the elements in the periodic table. Therefore, the ζ-factors for all these elements can be determined, while ignoring any X-ray absorption, if 30-nm-thick PE thin films are used.

As a demonstration of the ζ-factor method using PE standard, thin specimens, Fig. 3 shows the Al composition plotted against the specimen thickness determined from a nearly stoichiometric Ni_3Al thin film, which typically requires an absorption correction for Al K X-rays during quantification. The error bars represent 99% (3 σ) confidence limits. One of the major advantages of the ζ-factor quantification is the simultaneous thickness determination at the individual measured points. This analysis was performed using the VG HB 603 AEM at Lehigh University operated at 300 keV, equipped with a Faraday cup for *in-situ* probe-current measurements. Pure Al and Ni thin films were used as the standards for this analysis (which don't require an absorption correction for the ζ-factor determination). These PE thin films were fabricated by evaporation and thicknesses were determined using a profilometer. The measured thicknesses of the Al and Ni films were 80 ± 5 and 66 ± 5 nm, respectively. The corresponding ζ-factor values determined from these films were 1555 ± 53 kg·electron/(m^2·photon) for Al and 1194 ± 13 kg·electron/(m^2·photon) for Ni. In Fig. 3, the solid line and shadowed range represent the average composition with 99% confidence limits determined independently from a bulk Ni_3Al sample in an EPMA. The compositions determined via the ζ-factors superimpose well on the EPMA data over the thickness range relevant to this analysis.

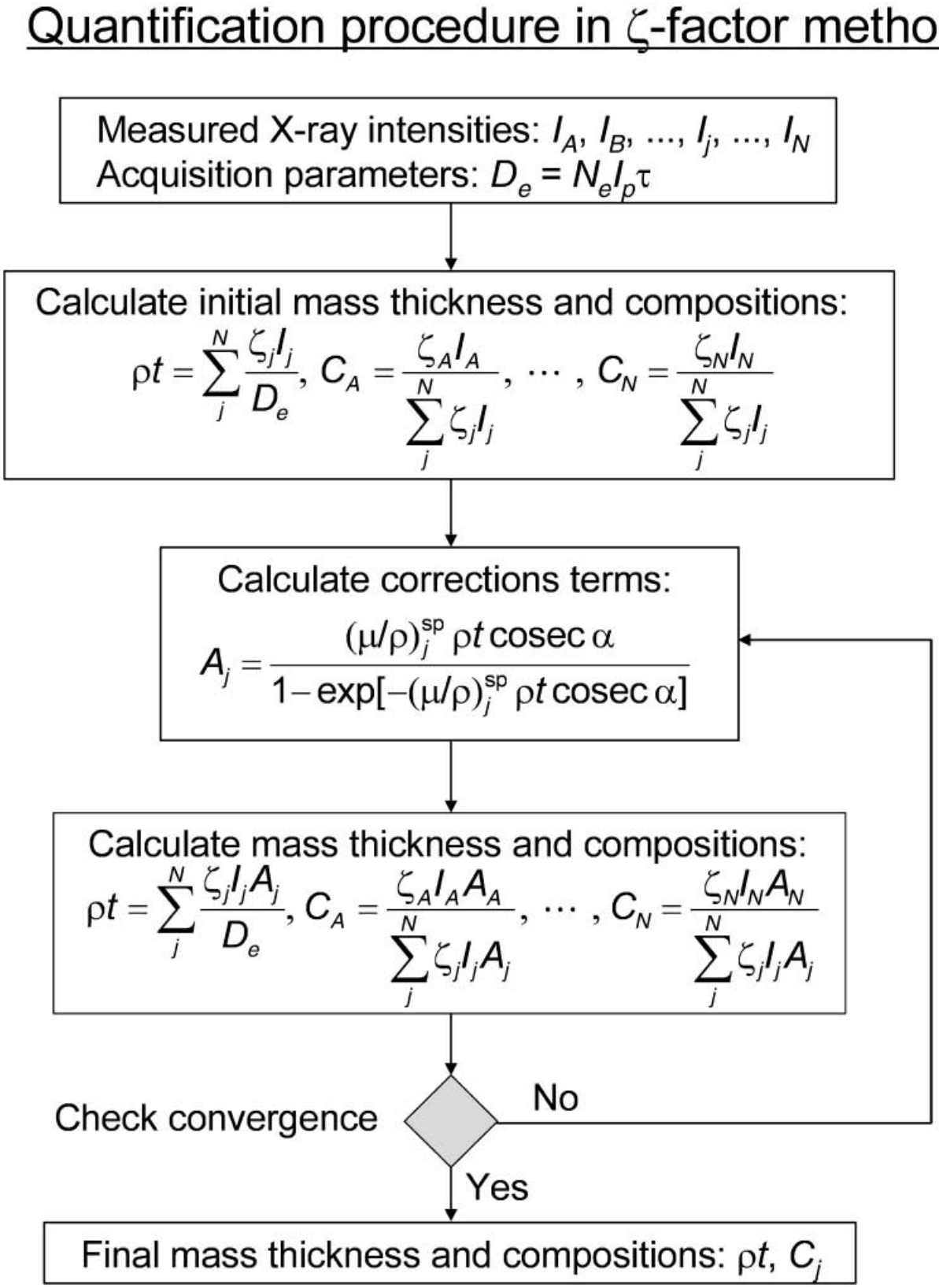

Fig. 1. A flow chart of quantification procedure in the ζ-factor method with the X-ray absorption correction.

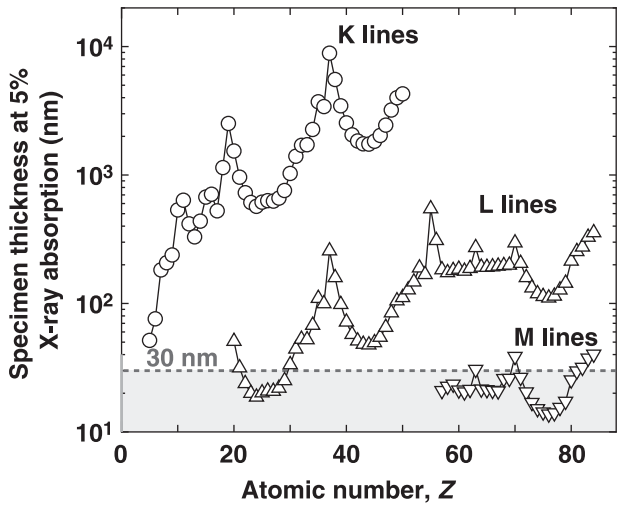

Fig. 2. The critical specimen thickness at 5% X-ray absorption in the pure element thin films. The shadowed area indicates the specimen thickness range below 30 nm. The critical thicknesses at the 5% absorption for all the K line and most of the L lines above Zn (> ~1 keV) are higher than the 30 nm.

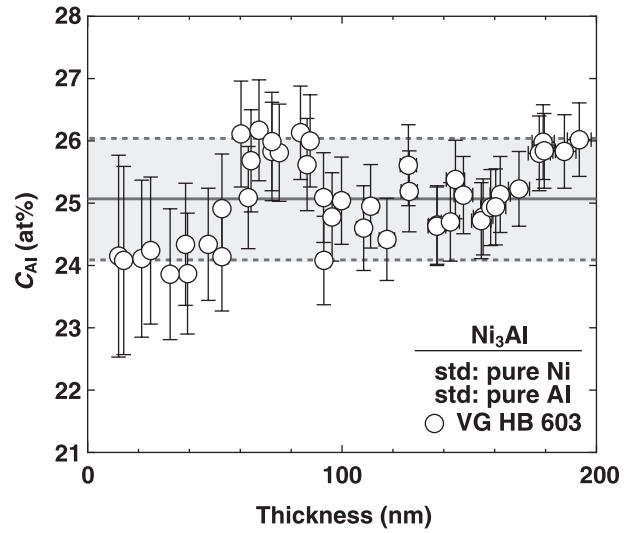

Fig. 3. The Al composition plotted against the specimen thickness determined from a nearly stoichiometric Ni_3Al thin film by the ζ-factor method in the VG HB 603 analytical electron microscope. As standards for this quantification, pure element Al and Ni thin films were used. The error bars represent 99% (3 σ) confidence limits. The solid line and shadowed range represent the average composition and its 99% confidence limit determined independently from the bulk Ni_3Al sample by an electron probe microanalyser.

It should be noted that other attempts have been made to replace multielement-alloy standards with PE thin films (Philibert *et al.*, 1970; Brown *et al.*, 1981; King, 1985). These approaches are similar to the ζ-factor method as they all use the X-ray production rate in their definition, i.e. simultaneous beam-current measurement is essential. The major difference from the ζ-factor method is that the previous PE standard approaches all employ the Cliff-Lorimer method for quantification. Unfortunately, the previous PE-standard approaches did not gain widespread acceptance despite the easier fabrication of PE films. One of the major reasons for the unpopularity was the requirement for beam-current measurements. The beam currents were not stable in early AEMs and, more importantly, an in-column Faraday cup was not available (and is still not integrated into any commercial AEM). Therefore, it was very difficult to determine the X-ray production rate accurately enough for quantification in those AEMs, although the specimen thickness of the PE films can be measured more accurately. Solving the beam-current measurement problem is clearly critical to the future success of the ζ-factor approach and this will be discussed later in this work.

In addition to the PE-film approaches, quantification procedures for thin specimens via bulk standards were also proposed (Philibert & Tixier, 1975; Thomas *et al.*, 1984; Boon & Bastin, 2004). It is obviously much easier to prepare bulk standards but full, matrix-correction procedures were still required to determine the X-ray production rate and these procedures are more complicated and sophisticated than Eq. (2). Furthermore, the operating conditions (e.g. kV or beam current) for bulk samples were difficult to keep similar to those for thin films in AEMs because of the significant difference in the X-ray production between the thin specimens and bulk samples.

Use of universal thin-film standards

The PE thin films are more routinely generated than the multielement, thin-film standards for *k*-factor determination. When quantitative analysis is performed on unknown multielement systems, the ζ-factor determination is still tedious because the ζ-factors for all the elements in the systems are required, which is the same limitation as the Cliff-Lorimer method. However, it is not even necessary to acquire a series of the PE thin films because an entire set of ζ-factors for K-shell X-ray lines can be estimated from a single spectrum (Watanabe & Williams, 1999a) generated from the NIST thin-film, glass, SRM 2063 (Rasberry, 1987). Note that SRM 2063 is the only available thin-film standard (containing Mg, Si, Ca, Fe and O) and has the advantage that its composition is known to a high degree of accuracy, as are its thickness and density. NIST has reissued a thinner version of SRM 2063, termed SRM 2063a (Reed, 1993a). The SRM 2063/2063a thin film was originally designed for the *k*-factor determination (Steel *et al.*, 1981, 1997).

By measuring a single spectrum from an SRM 2063/2063a thin film, the ζ-factors of Mg, Si, Ca, Fe and O can be determined for windowless (WL) and ultra-thin window [including atmospheric thin window (ATW)] XEDS systems. The ζ-factors for other elements can then be estimated by inter/extrapolation from the five measured ζ-factors [it should be noted that this approach is based on Zemyan's parameter-optimization

determination of a series of *k*-factors (Zemyan, 1995; Williams *et al.*, 1998)]. For accurate inter/extrapolation, the measured ζ-factors need to be fitted by optimizing several uncertain parameters associated with the X-ray generation and detection, such as the ionization cross-section and the thicknesses of detector-window materials for the detector efficiency term ε_A. These uncertain parameters can be obtained by minimizing the following χ^2 value by the optimization (e.g. Press *et al.*, 2002; Galassi *et al.*, 2002)

$$\chi^2 = \sum_j \left(\frac{\zeta_j^{\exp} - \zeta_j^{\mathrm{cal}}}{\Delta\zeta_j^{\exp}} \right)^2 \qquad (10)$$

where $\zeta^{\exp}$ and $\Delta\zeta^{\exp}$ are the measured ζ-factor and associated error (standard deviation), respectively, and ζ^{cal} is the theoretically calculated ζ-value from Eq. (5). To determine the uncertain parameters by fitting properly to the measured ζ-values, two important parameters should be incorporated into Eq. (5): (1) a scaling factor for the ionization cross-section *Q* as the absolute magnitude of the cross-section may deviate from the real case and (2) an ice-layer thickness that must be included in the detector efficiency term in addition to the original window materials because an ice layer may build up in front of the window in any XEDS detector interfaced to an AEM (e.g. Foitzik *et al.*, 1993; Michael, 1995).

In addition to these parameters, many models for the ionization cross-section are available. Too many choices of *Q* can be another uncertainty in parameter optimization. In order to select the best model, a parameter optimization was performed with the various *Q* models to fit the ζ-factors measured from SRM 2063a in two different AEMs: (1) a VG HB 603 300-keV AEM equipped with an Oxford WL XEDS detector [$\Omega = 0.30$ sr (Lyman *et al.*, 1994)], immediately after conditioning for de-icing and (2) a JEOL JEM-2010F 200-keV AEM with a Thermoelectron ATW XEDS detector [$\Omega = 0.13$ sr (Okamoto *et al.*, 2003)]. In these optimizations, the scaling factors for *Q* and thicknesses of the ice, Au contact and Si dead layer were fitted. For the ATW detector in the JEM-2010F, however, nominal thicknesses were used for the polymer thin window coated with Al (Moxtek AP1.3; detailed specifications can be found at www.moxtek.com) as only up to four parameters can be fitted from the five measured ζ-factors. For calculation of the detector efficiency term, a source code of DESKTOP SPECTRUM ANALYSER software (Fiori *et al.*, 1992) was modified into C++ and incorporated into the parameter-fitting program. In addition, the following data were used for the parameter optimization: the mass absorption coefficients of Heinrich (1987), the relative intensity ratios of Fiori *et al.* (1992) and the fluorescence yields of Bambynek (1984). The results of the parameter optimization (scaling factors and χ^2 values) for the 22 *Q* models in the two AEMs are summarized in Table 1. Despite the fact that most of these *Q* models were proposed for 10–30-keV EPMAs, the χ^2 values obtained using the 200- and 300-keV AEMs are reasonably small. The χ^2 values obtained from the VG HB 603 tend to be smaller than those from the JEM-2010F. This is because the measured intensities of the O Kα and Mg Kα peaks are higher from the WL detector on the VG HB 603 than from the ATW detector on the JEM-2010F due to the higher detection efficiency in the lower-energy region of the spectrum. The scaling factor varies from 0.4 to 1.8 depending on which *Q* was used and proper parameter optimization was never performed without employing the scaling factor. In comparing the results in Table 1, the *Q* models of Powell (1976b), Schreiber & Wims (1981), Casnati *et al.* (1982), Zaluzec (1984), Jakoby *et al.* (1987) and Paterson *et al.* (1989) might be useful for general application.

Figure 4 shows the ζ-factors measured from the SRM 2063a specimen (open circles) in the VG HB 603 (Fig. 4a) and the JEM-2010F (Fig. 4b), plotted against the X-ray energy. The closed circles in Fig. 4 indicate a series of the ζ-factors estimated from the measured values by the parameter optimization. For the ζ-factor estimations in both AEMs, the cross-section model proposed by Paterson *et al.* (1989) was used. The error bars indicate 99% ($\pm 3\,\sigma$) confidence limits. The procedures to determine errors for both the measured and estimated ζ-factors will be described in the following section. As shown in Fig. 4(a) and (b), both sets of estimated ζ-factors agree well with the measured values. As a demonstration of the robustness of the technique, these estimated ζ-factors were used to quantify a Cu-5.7 at% Mn alloy (Williams *et al.*, 2002). The quantified results are shown in Fig. 5 where the determined Mn composition is plotted against the determined specimen thickness. In Fig. 5, the solid line and shadowed area between the dashed lines indicate the average composition of Mn and the 99% confidence limits determined from the bulk sample by an EPMA. The Mn compositions determined by the ζ-factor method superimpose well on the Mn composition measured by the EPMA even though neither Cu nor Mn is present in SRM 2063a. It should be noted that the deviation in the Mn composition at the thickness range < 20 nm is probably due to preferential sputtering during specimen preparation by Ar-ion polishing.

Error determination in the ζ-factor method

Errors in ζ-factor determination

Errors in an individual ζ-factor measurement. In general, if a function consists of n variables such as $f = f(p_1, p_2, \ldots, p_n)$, the error in *f*, σ_f, can be given from the errors in the individual variables, σ_{pj} (Lyons, 1991)

$$\sigma_f^2 = \sum_{j=1}^{n} \left(\frac{\partial f}{\partial p_j} \right)^2 \sigma_{p_j}^2 \qquad (11)$$

To satisfy the above equation, the individual variables must be uncorrelated. In Eq. (2), the variables for a single ζ-factor measurement are the composition of the standard (*C*) the X-ray intensity (*I*) and the specimen thickness (*t*) [or more generally

Table 1. Summary of the scaling factor and the χ^2 value for different ionization cross-section models obtained from the ζ-factor estimation in the VG HB 603 and JEM-2010F analytical electron microscopes.

Cross-section model for K-shell ionization	VG HB 603 300 keV, WL XEDS		JEOL JEM-2010F 200 keV, ATW XEDS	
	Scaling factor	χ^2 value	Scaling factor	χ^2 value
Fabre (1949)	0.924 ± 0.023	1.345	0.849 ± 0.021	1.659
Mott & Massey (1949)	1.801 ± 0.046	1.252	1.211 ± 0.030	1.997
Worthington & Tomlin (1956)	1.801 ± 0.046	1.252	1.211 ± 0.030	1.997
Drawin (1961)	1.111 ± 0.028	1.304	0.761 ± 0.019	1.719
Green & Cosslett (1961)	1.256 ± 0.032	1.291	0.858 ± 0.021	1.745
Gryzinski (1965)	1.294 ± 0.031	1.331	0.856 ± 0.021	2.326
Kolbenstvedt (1967)	0.735 ± 0.012	1.328	0.585 ± 0.015	2.336
Lotz (1967)	0.998 ± 0.025	1.290	0.682 ± 0.017	1.745
Brown (1974), Powell (1976a)	1.313 ± 0.033	1.251	0.900 ± 0.022	1.987
Powell (1976b)	0.952 ± 0.024	1.360	0.657 ± 0.016	1.642
Quarles (1976)	0.625 ± 0.016	1.309	0.513 ± 0.012	1.720
Schreiber & Wims (1981)	0.780 ± 0.020	1.656	0.555 ± 0.014	1.638
Casnati *et al.* (1982)	0.569 ± 0.014	1.363	0.465 ± 0.011	1.641
Ogilvie (1984)	1.761 ± 0.032	1.402	1.442 ± 0.036	2.396
Zaluzec (1984)	0.632 ± 0.016	1.833	0.533 ± 0.013	1.569
Jakoby *et al.* (1987)	0.618 ± 0.015	1.628	0.503 ± 0.056	1.570
Paterson *et al.* (1989)	0.929 ± 0.023	1.323	0.759 ± 0.019	1.694
Pouchou & Pichoir (1991)	0.861 ± 0.021	1.966	0.638 ± 0.016	1.592
Pouchou (1994)	0.861 ± 0.021	1.966	0.638 ± 0.016	1.592
Deutsch *et al.* (1994)	0.536 ± 0.010	1.502	0.429 ± 0.011	2.515
SIGMAK2 (Egerton, 1986)	0.631 ± 0.016	1.242	0.489 ± 0.012	1.843
SIGMAK3 (Egerton, 1996)	0.642 ± 0.016	1.266	0.496 ± 0.012	1.833

ATW, atmospheric thin window; WL, windowless; XEDS, X-ray energy dispersive spectrometry.

the mass-thickness (ρt)]. Therefore, the error in the ζ-factor from a single measurement can be derived from Eqs (2) and (11)

$$\Delta\zeta = \left[\left(\frac{\Delta C}{C}\right)^2 + \left(\frac{\Delta I}{I}\right)^2 + \left(\frac{\Delta t}{t}\right)^2\right]^{1/2} \zeta \qquad (12)$$

where ΔC, ΔI and Δt indicate the errors in C, I and t, respectively. Both ΔC and Δt should be determined by an independent analysis of the standard specimen beforehand (note that the $\Delta C/C$ term is negligible when a PE thin film is used). The ΔI term is given by $\nu\sqrt{I}$ if the counting statistics of the measured X-ray intensity obey the Poisson distribution (e.g. Thompson, 2001) and ν is a factor depending on which confidence limit is chosen (i.e. $\nu = 1$ for a 68% confidence limit, $\nu = 2$ for 95%, $\nu = 3$ for 99%, etc.). Note that the Poisson distribution approaches the Gaussian distribution as the intensity increases. Obviously the confidence limits for all the variables should be selected consistently.

Errors in a series of ζ-factor measurements. To improve statistical accuracy, X-ray intensities should be measured several times from a standard specimen for the ζ-factor determination (in a similar manner to *k*-factors). The error in the ζ-factor after m measurements can be expressed as (e.g. Kreyszig, 1999)

$$\Delta\zeta = t_\alpha^{m-1}\sqrt{\frac{s^2}{m}} \qquad (13)$$

where t_α^{m-1} is the Student's t value at the given confidence limit (e.g. 99%) of m measurements and s^2 is the variance of m measurements, given as

$$s^2 = \sum_{j=1}^{n} \frac{(\zeta_j - \bar{\zeta})^2}{n-1} \qquad (14)$$

where $\bar{\zeta}$ is the average value after m measurements. When a standard thin film with homogeneous thickness such as the PE film is used for the ζ-factor determination, each error in the individual measurements should be similar. As long as the individual error values are similar, the above equation can be used to evaluate the total error in the process.

However, if local thickness varies in a standard specimen (such as a wedge-shaped specimen), then individual error values can be significantly different as the errors from the thickness and the intensity may vary significantly. In this situation, the influence of the errors in the individual ζ-factor measurements needs to be taken into account using weighting factors. The average value of the ζ-factor weighted by the individual errors can then be expressed as (e.g. Galassi *et al.*, 2002)

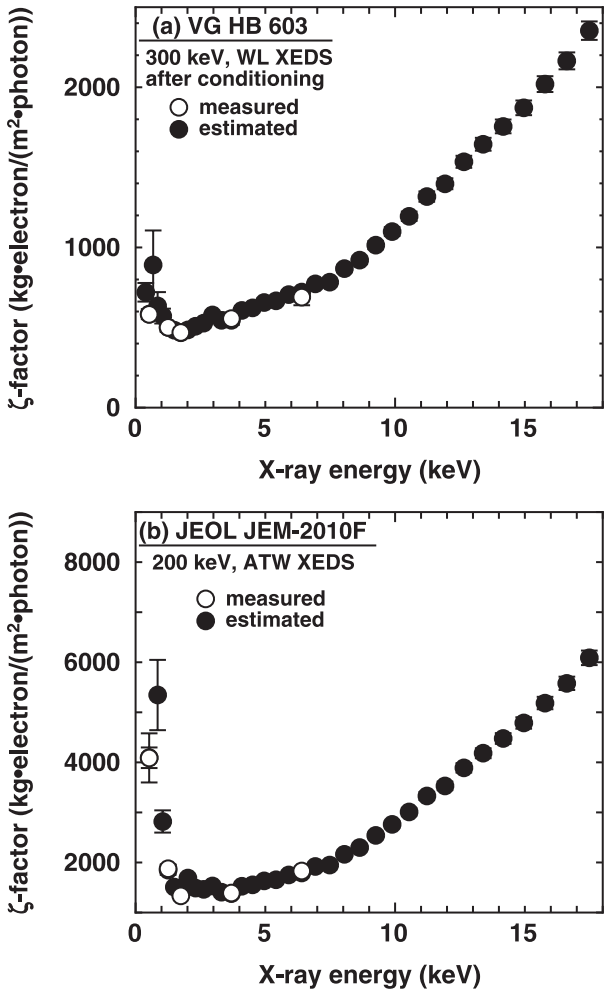

Fig. 4. The ζ-factors of K lines plotted against the X-ray energy. ○, measured values from the SRM 2063a glass thin-film; ●, estimated values by fitting to the measured values. Results by (a) a VG HB 603 300-keV analytical electron microscope (AEM) equipped with an Oxford windowless (WL) X-ray energy dispersive spectrometry (XEDS) detector (X-ray collection angle of 0.30 sr) and (b) a JEOL JEM-2010F 200-keV AEM with a Thermoelectron atmospheric thin window (ATW) detector (0.13 sr).

$$\bar{\zeta} = \frac{\sum_{j=1}^{n} w_j \zeta_j}{\sum_{j=1}^{n} w_j}, \quad w_j = \frac{1}{\Delta\zeta_j} \tag{15}$$

and the weighted variance is also given as

$$s^2 = \frac{\sum_{j=1}^{n} w_j}{\left(\sum_{j=1}^{n} w_j\right)^2 - \sum_{j=1}^{n} (w_j)^2} \sum_{j=1}^{n} w_j (\zeta_j - \bar{\zeta})^2 \tag{16}$$

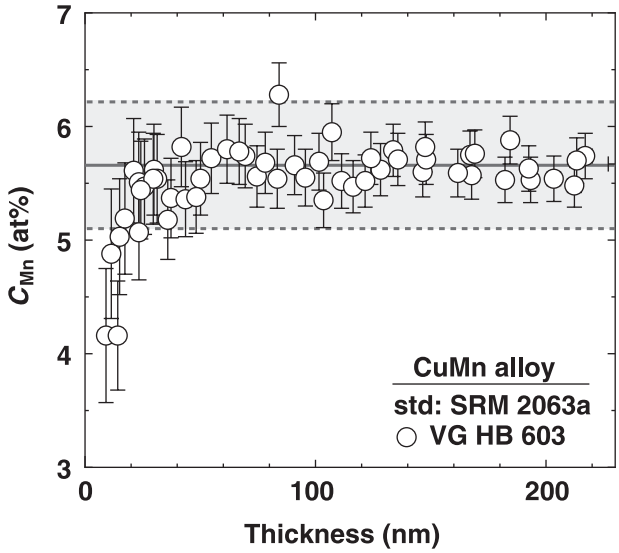

Fig. 5. A plot of the Mn composition in a Cu-5.7 at% Mn alloy vs. specimen thickness measured in a VG HB 603 analytical electron microscope (Williams *et al.*, 2002; Fig. 10, reproduced by permission of Oxford University Press). Each composition was determined using the ζ-factors estimated from the SRM 2063a. The solid line and shadowed range represent the average composition and its 99% confidence limit determined independently from the bulk Cu-5.7 at% Mn alloy by an electron probe microanalyser.

The total error in the ζ-factor, for the general case, can be obtained from Eq. (14) by substituting Eqs (15) and (16).

Errors in the ζ-factor estimation. In the ζ-factor estimation from the universal standard, described in the previous section, several variables such as a scaling factor for Q and thicknesses of detector-window materials are adjusted by a numerical optimization. For this optimization, several ζ-factor values, determined with experimental errors, are required. The optimization to minimize the χ^2 value in Eq. (10) must be performed by iteration. Unfortunately, it is not straightforward to evaluate the errors in the fitting parameters and hence those of the estimated ζ-factors. Even in the iteration process, however, the errors can be calculated by an alternative approach (Lyons, 1991). Let the ζ-factors determined experimentally from the universal standard be denoted as ζ_j ($j = 1, 2, \ldots$). The corresponding errors $\Delta\zeta_j$ and fitting parameters q_i ($i = 1, 2, \ldots$) can be expressed as functions of ζ_j: $(q_1, q_2, \ldots, q_i, \ldots) = f(\zeta_1, \zeta_2, \ldots, \zeta_j, \ldots)$. The errors for q_i can then be calculated as follows:

1 the error-free q_i values are determined from the error-free ζ-factors;
2 the fitting parameters with the error contribution from the j^{th} ζ-factor, $q_i(\Delta\zeta_j)$, are calculated by substituting $\zeta_j + \Delta\zeta_j$ for ζ_j and
3 the errors of the fitting parameters Δq_i can then be obtained as

$$\Delta q_i = \sqrt{\sum_j [q_i(\Delta\zeta_j) - q_i]^2} \tag{17}$$

It should be noted that the individual ζ-factors should not be correlated with one another in order to satisfy Eq. (17). After the determination of the errors in the fitting parameters, the errors in the estimated ζ-factors can be calculated with the error values of q_i

$$\Delta\zeta_j^{\mathrm{cal}} = \sqrt{\sum_i [\zeta_j^{\mathrm{cal}}(\Delta q_i) - \zeta_j^{\mathrm{cal}}]^2} \tag{18}$$

where ζ_j^{cal} is the j^{th} ζ-factor estimated from the error-free q_i (and hence the error-free ζ-factor). $\zeta_j^{\mathrm{cal}}(\Delta q_i)$ is the ζ-factor calculated by substituting $q_i + \Delta q_i$ for q_i, which is only influenced by the error in q_i.

Errors in composition and thickness determinations

For quantification of unknown specimens via the ζ-factors, errors in the individual ζ-factors and X-ray intensities from each measured point must be taken into account. When X-ray absorption is negligible, as in more general cases, numerical iteration is required to determine the composition and thickness, as described above. Therefore, the alternative error estimation could be useful for quantification via the ζ-factors:

1 the error-free composition C_j and thickness t are determined from the error-free inputs;
2 with the k^{th} error contribution of the ζ-factor or of the X-ray intensity, compositions and thickness are calculated by substituting $\zeta_k + \Delta\zeta_k$ for ζ_k or $I_k + \Delta I_k$ for I_k, respectively and
3 the errors in the compositions and thickness are given as

$$\Delta C_j = \sqrt{\sum_{k=1}^{n} [C_j(\Delta\zeta_k) - C_j]^2 + \sum_{k=1}^{n} [C_j(\Delta I_k) - C_j]^2}$$
$$\Delta t = \sqrt{\sum_{k=1}^{n} [t(\Delta\zeta_k) - t]^2 + \sum_{k=1}^{n} [t(\Delta I_k) - t]^2} \tag{19}$$

If an n-component system is analysed, extra calculations to determine error-influenced values need to be performed 2n times (i.e. n times for individual ζ-factors and n times for individual measured X-ray intensities) after determination of the error-free values. This alternative error estimation approach seems tedious. However, the method is applicable to any calculation and requires iteration, similar to a matrix correction used for bulk sample analysis in an EPMA and any type of numerical optimizations. Therefore, there is no excuse not to perform the error analysis in quantification. Lastly, all these procedures for error analyses in the ζ-factor method are easily built into the computer software, which is available from the corresponding author.

Major advantages of the ζ-factor method for quantitative analysis

There are several advantages of the ζ-factor method over the Cliff-Lorimer ratio method. In this section, some of these advantages, mainly due to the availability of simultaneous thickness determination, are highlighted by specific examples.

Light-element analysis

The two major problems for quantitative light-element X-ray analysis are poor X-ray detection efficiency and significant X-ray absorption (e.g. Statham, 1998). The former issue can be compensated to some degree if an ultra-thin window or WL XEDS detector is used. However, the latter problem can be severe, especially when thin specimens that contain light elements [which only produce soft X-rays below 1 keV (< Na)] are analysed, e.g. many important oxide, carbide and nitride systems (such as most commercial ceramics). Unfortunately, the quantification of these materials in AEMs is more difficult using XEDS than using electron energy-loss spectrometry (EELS). Conversely, EELS analysis is also challenging if the specimen contains both light and very heavy elements together, such as Pb-based oxides. Therefore, as long as the X-ray intensities are detectable from those light elements, it would be ideal to perform quantitative analysis. In the ζ-factor method, the X-ray absorption correction is incorporated as described above and the ζ-factor method has already been shown to work well for several light-element (oxide) quantifications, even for the difficult Pb-based oxides (Gorzkowski *et al.*, 2004).

There is another standard thin specimen available for AEM. The NiO standard is well suited for characterization of the AEM–XEDS interface by measuring hole-counts and Ni K : L intensity ratios (the commercial version is designated as NiOx™, Egerton & Cheng, 1994; Bennett & Egerton, 1995). Figure 6 shows the oxygen composition and thickness measured individually from a 50-nm-thick NiOx by the VG HB 603 (circles) and JEOL JEM-2010F (triangles) AEMs, respectively. The acquisition conditions to obtain similar amounts of the Ni Kα intensity were 50 s with 0.5 nA for the VG HB 603 and 50 s with 1.0 nA for the JEM-2010F. For these quantifications, the ζ-factors were estimated from the SRM 2063a thin specimen (Fig. 4) and the thickness was deduced from the mass-thickness using an actual instead of a calculated NiO density. The shadowed areas in the composition and thickness indicate the ranges of ±1 at% and of ±5 nm, respectively. The individual analysis results from the VG HB 603 AEM are almost identical and the fluctuation ranges are ±1 at% and ±2 nm in 25 measurements. Conversely, the results from the JEM-2010F are more scattered both in the composition (±3 at%) and thickness (±6 nm). The differences in the data from the two AEMs are caused by the differences in the X-ray collection efficiency, i.e. the X-ray collection angles and the detector efficiencies at the O Kα peak (0.522 keV) are 0.30 sr and 0.58 for the VG HB 603 and 0.13 sr and 0.23 for the JEM-2010F, respectively (the details of how to determine the detector efficiency will be described later). The difference in the X-ray collection efficiency results in a 3× difference in the O Kα intensity (~7500 counts in the VG HB 603 and ~2500 counts

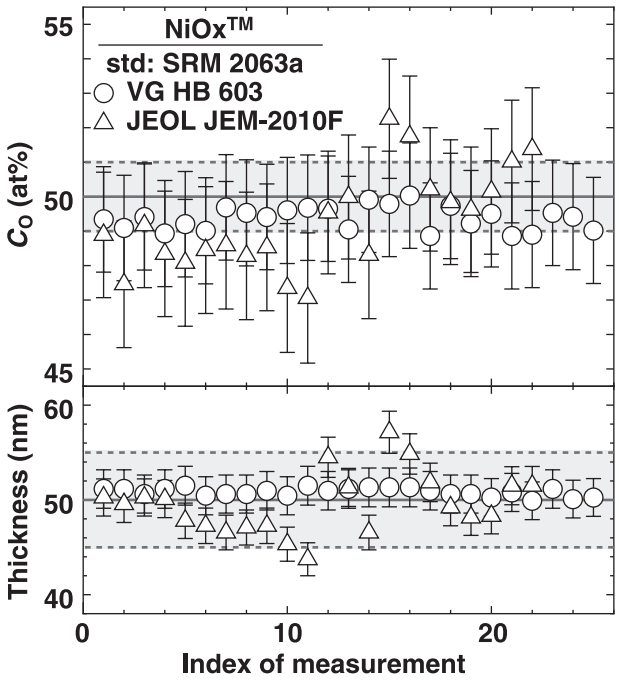

Fig. 6. Quantification results of the 50-nm-thick NiOx™ thin film by the ζ-factor method in VG HB 603 (○) and JEM-2010F (△). The determined composition and thickness are plotted against an index of individual measurements in the upper and lower parts, respectively. The shadowed areas indicate the ranges of ±1 at% and of ±5 nm, respectively.

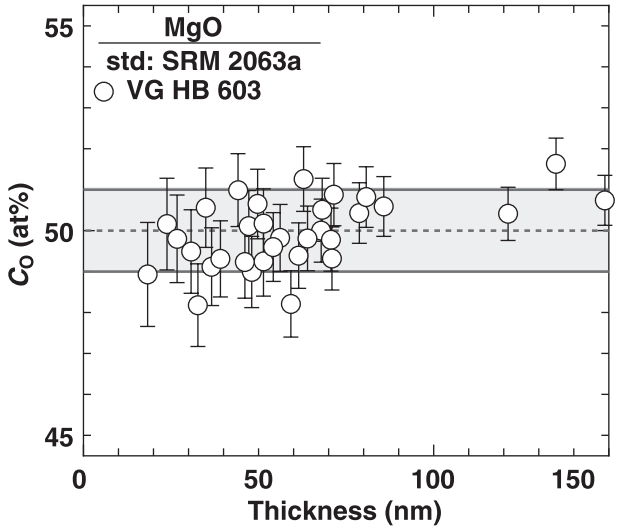

Fig. 7. Quantification results of MgO cuboids in VG HB 603; determined composition is plotted against determined thickness. The shadowed area indicates the range of ±1 at%.

in the JEM-2010F) even though the total Ni Kα intensities are similar (~25 000 counts). Therefore, even small fluctuations in the O Kα intensity in the JEM-2010F cause relatively large deviations in the determined composition and thickness. Despite these differences, one conclusion can be drawn from Fig. 6, i.e. the thickness determination by the ζ-factor method is very accurate.

Figure 7 shows another example of light-element analysis by the ζ-factor method: the oxygen composition determined from MgO cuboids in the VG HB 603, plotted against the specimen thickness determined via an actual density value. As the composition of MgO does not deviate from stoichiometry (i.e. Mg : O = 50 : 50) similar to NiO, it is easy to confirm the accuracy of quantification. The shadowed region indicates that the composition range deviated from stoichiometry by ±1 at%. Several results are slightly out of the shadowed range. However, most results lie in the shadowed area and even the worst results are still within ±2 at%. Due to the built-in absorption correction, quantitative analysis of light-element materials such as ceramics is routinely possible via the ζ-factor method. In the previously proposed absorption-correction procedures, such as the extrapolation method or the K : L intensity-ratio method, it is more difficult to quantify the MgO point-by-point. This is because multiple measurements are required for the extrapolation method and the K : L intensity ratio method is not applicable if there is no L-line emission.

It should be mentioned that the X-ray absorption correction can be performed if the thickness information can be obtained independently, e.g. by EELS. Recently, a light-element analysis method for X-ray analysis has been proposed in combination with EELS (Banchet *et al.*, 2003). In this approach, X-ray absorption correction can be performed via the relative thickness (the thickness divided by the mean free-path) and not via the absolute thickness. As the mean free-path is the major uncertainty for thickness determination for materials of unknown composition in EELS, this approach may produce a more accurate absorption correction than the use of other independent thickness-determination methods but is obviously not an improvement over PE thin films or use of the known 2063/2063a standard.

Determination of spatial resolution

Knowledge of the spatial resolution of analysis is important when elemental distributions need to be known, e.g. impurity segregant distributions around grain boundaries and constituent composition changes across interfaces. Many theoretical and experimental studies (see a summary in Williams & Carter, 1996) have been conducted to determine the analytical spatial resolution *R*. Williams *et al.* (1992) concluded that the calculation of *R* is limited by having to know the specimen thickness beforehand. However, the ζ-factor method gives the specimen thickness simultaneously with the compositions. Therefore, prior knowledge of thickness is no longer a limitation for the calculation of *R*, if the ζ-factor method is used.

The analytical spatial resolution *R* is strongly related to the interaction volume between the incident beam and the specimen, and hence the calculation of *R* requires information

about the incident beam size and the beam broadening. One of the most popular approaches to define the spatial resolution is to use the diameter at the midpoint of the truncated cone defined by the incident and exit beam diameters (Michael *et al.*, 1990; Williams *et al.*, 1992). This approach employs a single-scattering model (Goldstein *et al.*, 1977; Reed, 1982) to describe the beam broadening and gives good agreement between experimental and simulated results (Williams *et al.*, 1992), in spite of neglecting the electron intensity distribution in the incident beam or in the interaction volume. Recently, Keast & Williams (2000) evaluated various beam-broadening models by fitting to segregation profiles across grain boundaries and concluded that the Gaussian beam-broadening model (Doig *et al.*, 1980; Doig & Flewitt, 1982) is the best description of the interaction volume. The spatial resolution based on the Gaussian beam-broadening model was proposed by Van Cappellen & Schmitz (1992)

$$R = q[\sigma^2 + \beta(\kappa t)^3/2]^{1/2} \qquad (20)$$

where the scaling parameters q and κ are dependent on the chosen fraction of the incident intensity (e.g. $q = 4.29$ and $\kappa = 0.68$ for the spatial resolution that contains 90% of the incident intensity, which corresponds to the beam diameter at a thickness of $0.68t$ from the top surface). The terms σ and β are associated with the incident-beam size and the beam broadening, respectively, and are given by

$$\sigma = d_{TM}/4.29, \quad \beta = 500\left(\frac{4\bar{Z}}{E_0}\right)^2\left(\frac{\rho}{\bar{M}}\right) \qquad (21)$$

where d_{TM} is the incident beam diameter at full-with-tenth-maximum, E_0 is the incident beam energy (in eV) and $\bar{Z}$ and $\bar{M}$ are the averaged atomic number and atomic weight, respectively. As all the terms related to the specimen are determined by the ζ-factor method, R can be easily extracted at individual measured points if d_{TM} and E_0 are known. It should be noted that the thickness information via XEDS is also useful to determine segregation enrichments, not only for point analyses (Watanabe & Williams, 2003) but also for the box-scan approach (Alber *et al.*, 1997).

To demonstrate the efficacy of the ζ-factor method in spatial resolution determination, a set of quantitative X-ray maps around an α-Fe/Fe_3P interface in an Fe-17at% P alloy, obtained in the VG HB 603 AEM, is shown in Fig. 8. The annular dark-field scanning transmission electron microscopy (STEM) image is shown in Fig. 8(a) and the X-ray maps were acquired for a dwell time of 200 ms with 128×128 pixels. By applying the ζ-factor method, not only quantitative compositional maps of Fe (Fig. 8b) and P (Fig. 8c) but also a specimen-thickness map (Fig. 8d) can be obtained. The elemental distributions are clear between the two phases and the specimen is slightly thinner in the α-Fe region, especially around the interface. Figure 8(e) shows a map of the absorption-correction factor for the P Kα line, A_P. As described in Eq. (8), the absorption-correction factor increases from 1 as the magnitude of X-ray absorption increases. In this case, as the X-ray maps were acquired from a relatively thin region (< 60 nm), the A_P term is not very high. However, A_P can be very high when much thicker regions are analysed. The spatial resolution R calculated from the composition and thickness information at the individual pixels using Eq. (20) is shown in Fig. 8(f). In this analysis, a 1.5-nm probe (full-width-tenth-maximum) was used. At the interface, the R-value is about 2 nm. Figure 9 shows composition and thickness profiles extracted from Fig. 8 by binning 20 pixels together along with the interface to improve counting statistics (equivalent to a 4-s acquisition). The R-value at the interface measured from this profile is about 3.5 nm, which is larger than the calculated value. This is probably due to the inclination of the interface to the incident beam in this region of the specimen.

Determination of analytical sensitivity

The analytical sensitivity, i.e. the minimum detection limit, is another important figure of merit. In AEMs, the detection limit is relatively poor because the generated signals are small, due to the reduced beam–specimen interaction volumes. Joy & Maher (1977) proposed two different types of the minimum detection definitions for thin-film analysis: (1) the minimum mass fraction (MMF), the smallest concentration of an element that can be detected and (2) the minimum detectable mass (MDM), the smallest amount of a material that can be detected. In X-ray analysis (as for most analytical techniques), the MMF is preferable as determination of the MDM is rather complicated.

Romig & Goldstein (1979) defined a criterion for a minimum detectable peak-intensity in an X-ray spectrum, which was derived from the description of X-ray emission by Liebhafsky *et al.* (1955). The criterion is

$$I > 3\sqrt{2B} \qquad (22)$$

where I is the characteristic X-ray peak intensity above the background integrated over a certain energy range and B is the corresponding background intensity that can be obtained by averaging the background intensities in pre- and postpeak energy-windows, identical in range to that over which I was measured. Again, the I and B-values represent the numbers of

Fig. 8. A series of X-ray maps around an α–Fe/Fe_3P interface measured in the VG HB 603 analytical electron microscope. These maps were quantified by the ζ-factor method. (a) annular dark-field scanning transmission electron microscopy (ADF-STEM) image; (b) Fe map; (c) P map; (d) thickness map; (e) map of absorption correction factor for P Kα; (f) spatial resolution map; (g) map of the minimum mass fraction (MMF) for P; (h) map of a number of P atoms and (i) map of the minimum detectable mass (MDM) for P.

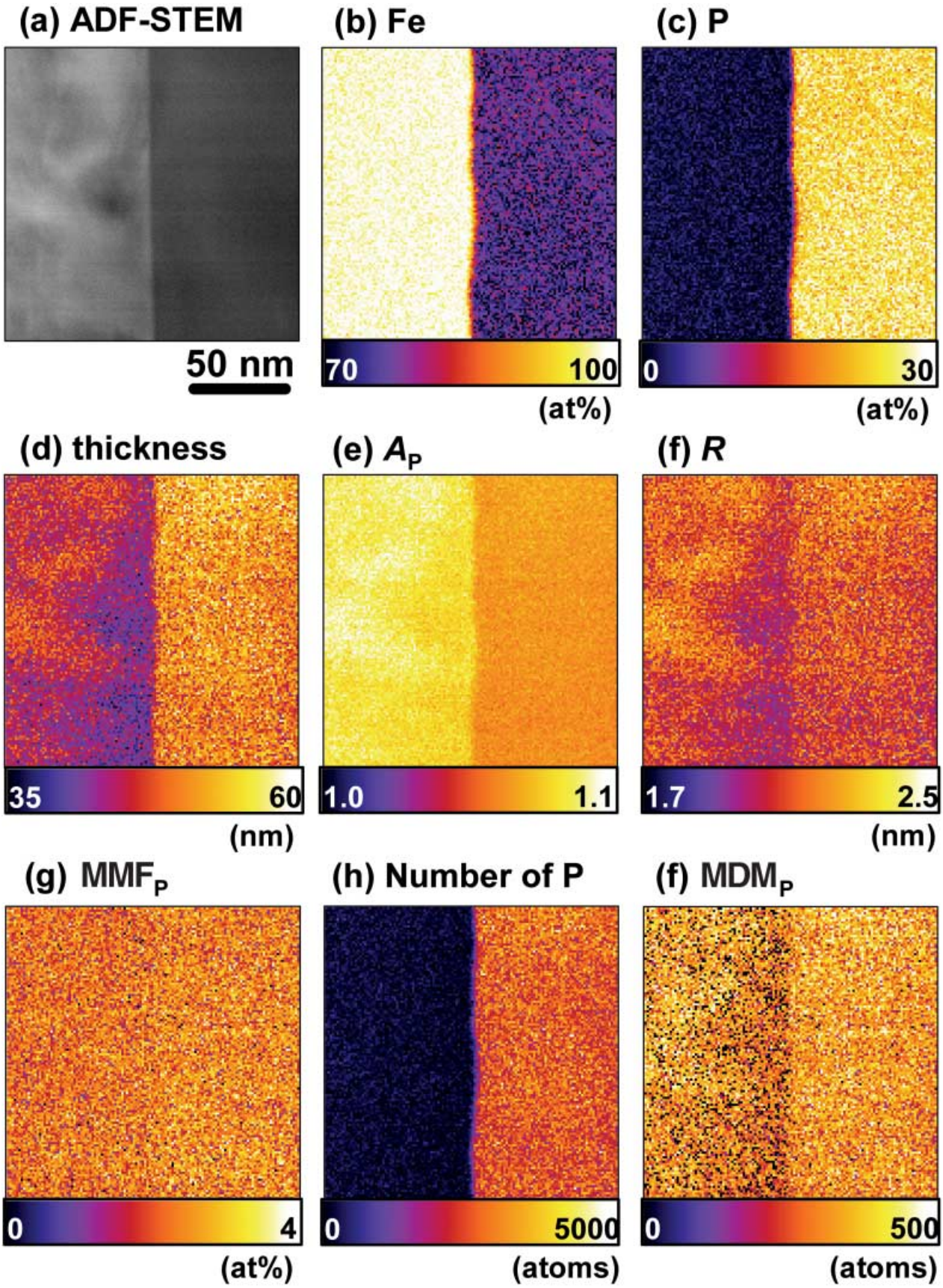

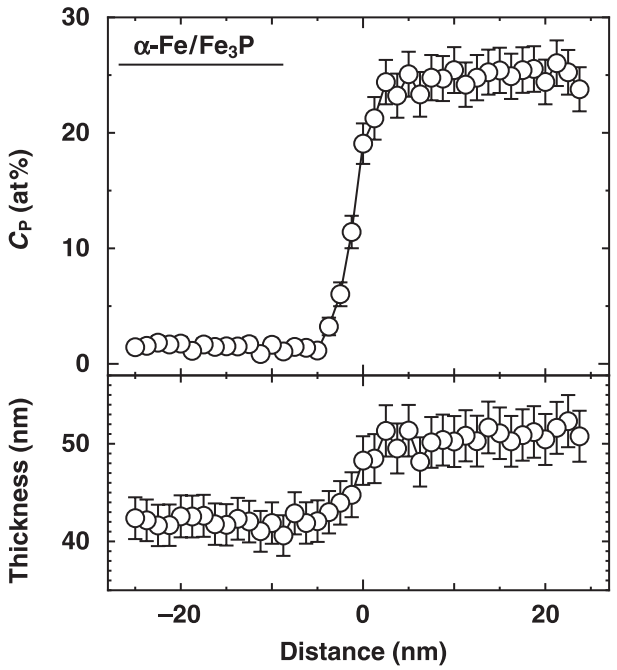

Fig. 9. The P concentration and thickness profiles extracted from the maps in Fig. 8 by binning 20 pixels along the interface to improve counting statistics.

the photons for the peak and background integrated in the same energy-window, respectively. When I is very small, the detectability of I is strongly influenced by the counting noise in the selected energy window, which is related to the standard deviation (1 σ) of $2B$ or $\sqrt{2B}$ as the total intensity in the selected energy window can be assumed as $2B$ ($\approx I + B$). Therefore, if the criterion, expressed in Eq. (22), is satisfied, the X-ray peak intensity is detectable with a ±99% confidence limit (3 σ). The MMF for thin-foil X-ray analysis was proposed by combining this criterion into the Cliff-Lorimer ratio equation (Romig & Goldstein, 1979; Michael, 1987). In a similar manner, this peak detection criterion can also be incorporated into the ζ-factor method and then the MMF can be expressed from Eq. (7) as

$$\mathrm{MMF}_A = \frac{\zeta_A 3\sqrt{2B_A}}{D_e \rho t} \qquad (23)$$

If X-ray absorption is not negligible, the absorption-correction term should be multiplied by the $3\sqrt{2B_A}$ term. Figure 8(g) shows the MMF map of P converted from the composition and thickness maps. The background intensity for the MMF calculation was obtained by averaging counts in pre- and postpeak energy windows. The energy windows for the P K peak, pre- and postpeak positions were 1.96–2.08, 1.56–1.68 and 2.24–2.36 keV, respectively. It should be noted that the MMF value given by Eq. (23) is defined in wt%. However, the wt% MMF can easily be converted to the at% MMF value. In this map, the MMF of P is ~2.5 at%, which is close to the P composition in the α-Fe matrix.

The MMF values of any analyses in AEMs are poor, due to the limited analysis volume. In contrast, another expression of the minimum detection is the MDM which, in AEMs, can be better than any other analysis technique (Williams & Carter, 1996), except for atom-probe field ion microscopy. The MDM can be defined as the number of atoms detectable in the analysis volume (Watanabe & Williams, 1999b). Due to the difficulties of determining the analysis volume, the MDM expression is rarely employed. However, if the ζ-factor method is used, the determination of the analytical volume (and hence the MDM) is no longer a limitation and can be performed at the individual measured points. As the beam diameter at the depth z can be expressed as $q(\sigma^2 + \beta z^3/2)^{1/2}$ in the Gaussian beam-broadening model (Van Cappellen & Schmitz, 1992), the analysis volume is given as

$$V = \int_0^t \pi[q(\sigma^2 + \beta z^3/2)^{1/2}/2]^2 \, dz = \frac{\pi q^2}{32}(8\sigma^2 t + \beta t^4) \qquad (24)$$

As long as the Gaussian beam-broadening model is used, the analysis volume V is defined as a function of the fraction of the total incident intensity, similar to the definition of the spatial resolution. To maintain the consistency in definitions, the fractional parameter q should be selected as 4.29 (corresponding to 90% of the total intensity). As the total number of atoms in the analysed volume is obtained from $N_v \rho V/\bar{M}$ (N_v, Avogadro's number), the number of atoms and the MDM for individual elements can be determined by multiplying individual compositions and MMF values in the atomic fraction, respectively. The results of this approach (i.e. number of atoms and the MDM) can also be used to form images, as shown in Fig. 8 (h, number of P atoms; i, MDM for P). In comparison to the MMF, the MDM is influenced by the specimen thickness. In these maps, the MDM of P is about 400 atoms. If the acquisition time and/or beam current were increased, both the MMF and the MDM would be improved. In summary, not only the compositions but also the specimen thickness and associated information can be visualized by combining X-ray mapping with the ζ-factor method.

Determination of detector efficiency and performance evaluation of X-ray energy dispersive spectrometry–analytical electron microscope interface

When a series of the ζ-factors is estimated from the NIST SRM 2063a thin specimen, several thicknesses of detector and window materials, which together determine the detector efficiency, must be fitted. Figure 10 shows another series of ζ-factors determined from SRM 2063a in the VG HB 603. These data were determined in the same session as shown in Fig. 4(a) but before the detector was conditioned to remove any ice build-up. In comparison with the results after detector conditioning, the ζ-factors are higher especially in the lower

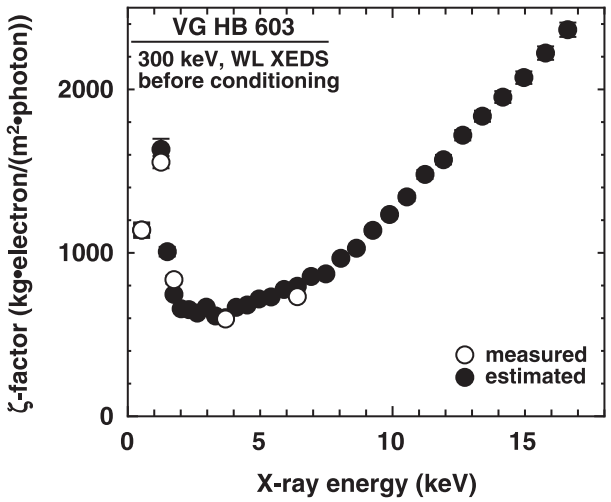

Fig. 10. The measured and estimated ζ-factors of K lines plotted against the X-ray energy. The ζ-factor determination was examined in the VG HB 603 analytical electron microscope with the windowless (WL) X-ray energy dispersive spectrometry (XEDS) detector before conditioning.

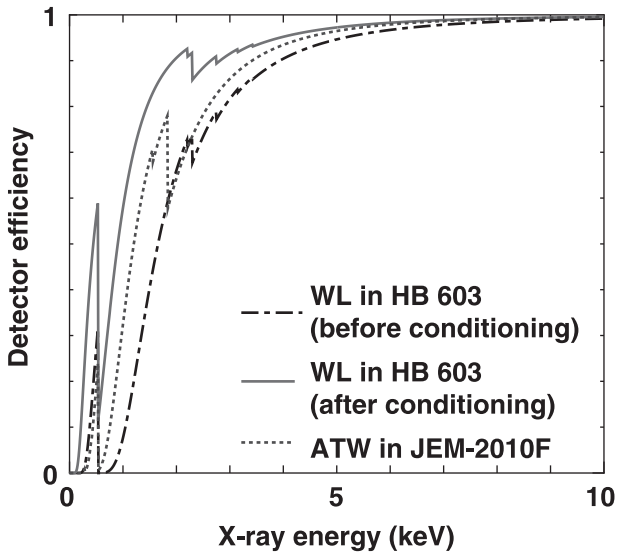

Fig. 11. The X-ray detector efficiency calculated from thickness information of the detector-window materials determined by the parameter optimization for the VG HB 603 analytical electron microscope (AEM) with the windowless (WL) X-ray energy dispersive spectrometry (XEDS) detector (before and after conditioning) and for the JEOL JEM-2010F AEM with the atmospheric thin window (ATW) XEDS detector, plotted against the X-ray energy.

X-ray energy regions because of the removal of ice build-up in front of the active area of the detector. The ice thickness determined from the ζ-factor estimation is summarized in Table 2. After conditioning, the ice thickness was less than 1 μm. However, it was over 5 μm before conditioning. The ice thickness for the ATW detector in the JEM-2010F was 2.2 μm. Therefore, the ice thickness needs to be considered for any ζ-factor estimation.

One advantage of the ζ-factor estimation is the determination of the several detector and window thicknesses, from which the detector efficiency can be derived. Figure 11 shows the detector efficiencies determined for the WL detector in the VG HB 603 (before and after conditioning) and the ATW detector in the JEM-2010F, plotted against the X-ray energy. For the calculation of the detector efficiency, thicknesses of the ice layer, Au-contact layer and Si dead layer (all determined in the ζ-factor estimation via the SRM 2063a thin specimen) were used. However, rather than performing such calculations for the other relevant detector dimensions (window materials and Si crystal thickness) nominal values, suggested by the manufacturer, were used. The detector efficiency for the WL detector can be worse than that for an ATW detector, if there is significant ice build-up, such that X-rays with energies slightly higher than the O K absorption edge (0.532 keV) are strongly absorbed. As the Mg K and O K lines are strongly influenced by the ice layer in the SRM 2063a, the ζ_{Mg} value can be used as a marker for the ice build-up. The measured ζ-factor values of the Mg K and Fe K lines are also summarized in Table 2. The ζ_{Mg} value is significantly changed (by more than 300%) before and after detector conditioning. In contrast, the ζ_{Fe} value, which is unaffected by the presence of ice, remains almost the same before and after conditioning but is different for the two different instruments. As expressed in Eq. (5), the ζ-factor is inversely proportional to the X-ray emission and detection rates. Therefore, a ζ-factor for a hard X-ray line such as ζ_{Fe} can be used to evaluate and monitor the AEM–XEDS

Table 2. Summary of the ice layer thickness and the determined ζ-factors of the Mg K and Fe K lines in different microscope conditions.

		ζ-factor [kg·electron/(m²·photon)]	
Instrument	Ice layer thickness (μm)	ζ_{Mg}	ζ_{Fe}
VG HB 603 with WL XEDS detector (before conditioning)	5.50 ± 0.19	1555 ± 38	733 ± 18
VG HB 603 with WL XEDS detector (after conditioning)	0.91 ± 0.16	500 ± 26	689 ± 50
JEOL JEM-2010F with ATW XEDS detector	2.07 ± 0.19	1874 ± 87	1831 ± 41

XEDS, X-ray energy dispersive spectrometry; ATW, atmospheric thin window; WL, windowless.

interface. If any particular instrument provides larger ζ_{Fe} values after installation or after major upgrades, there could be a problem in the AEM–XEDS interface such as wrong detector positioning or poor collimator alignment.

Discussion

Comparison with the Cliff-Lorimer ratio method

The advantages of the ζ-factor method over the traditional Cliff-Lorimer ratio method were described in the previous sections. These advantages are summarized as: (1) use of PE thin film standards; (2) built-in absorption correction; (3) calculation of the spatial resolution; (4) mapping of composition in terms of the absolute number of atoms and (5) determination of the MDM values. Compared with the previously proposed absorption-correction procedures, the absorption correction in the ζ-factor method is performed for individual measurements only using X-ray intensities and this is the most flexible and easy approach. In addition, the ζ-factor can also be used for diagnosis of problems with the AEM–XEDS interface in combination with the NIST SRM 2063a universal, standard, thin specimen. There are two major disadvantages to the new ζ-factor method: (1) the need for specimen-thickness information and (2) the requirement for measurement of the beam current. The former limitation can be simplified if PE thin films are used. Therefore, the capability for *in-situ* beam current measurement is a minimum requirement if the ζ-factor method is to be used.

If we take a ratio between Eqs (2) and (6) and rearrange it as

$$\frac{C_A}{C_B} = \frac{\zeta_A}{\zeta_B}\frac{I_A}{I_B} \tag{25}$$

by comparing the above equation with the original Cliff-Lorimer ratio equation [Eq. (1)], the following relationship holds between the Cliff-Lorimer *k*-factor and the ζ-factor

$$k_{AB} = \frac{\zeta_A}{\zeta_B} \tag{26}$$

This relationship between *k*- and ζ-factors permits conversion of a series of ζ-factors from an existing series of the *k*-factors, which have been determined in a particular instrument, by measuring only one ζ-factor, e.g. for Si K or Fe K. For accurate quantification, freshly measured ζ-factors are always recommended. However, conversion from the existing database of *k*-factors provides a basis for generating the ζ-factor values without having to perform a whole new range of experiments.

Limits of the ζ-factor method

Maximum applicable thickness. In thin-film specimens, the ionization cross-section is usually treated as a constant (part of the thin-film approximation). In other words, it is assumed that no energy loss occurs due to inelastic scattering of the incident electrons within the thin specimen (strictly speaking, neither characteristic X-rays nor energy-loss electrons can be generated if this condition applies, so it is somewhat unrealistic). Ignoring this lack of realism, it is assumed that the probability of inelastic-scattering events must increase as the specimen thickness increases. If the incident electrons lose significant energy, Eq. (5) [and hence Eq. (2)] no longer applies and the energy-loss term needs to be taken into account, which is not desirable as integration of the electron energy-loss means the whole procedure requires matrix-type corrections similar to those used in bulk-sample analysis. Therefore, the maximum thickness applicable for the ζ-factor method (at which energy-loss can still be neglected and Q can be treated as a constant) is discussed here.

The electron penetration range in the depth direction, z, is well defined in a bulk sample and derived from an integral of the energy-loss equation over a range from the incident energy E_0 down to zero energy (e.g. Reed, 1993b)

$$z = \int_0^{E_0} \frac{dE}{dE/dz} \tag{27}$$

If it is assumed that any electron energy loss below 3% of the incident electron energy is negligible in thin specimens, the maximum applicable thickness can be given by a modification to Eq. (27)

$$t_{\max} \equiv \int_{0.97E_0}^{E_0} \frac{dE}{dE/dz} \tag{28}$$

As the above integral is proportional to $E^{5/3}$ (Kanaya & Okayama, 1972), $t_{\max} = (1^{5/3} - 0.97^{5/3})z = 0.0495z$, i.e. only ~5% of the whole electron penetration range can be defined as the maximum thickness for negligible electron energy loss. From the Kanaya-Okayama electron range with the relativistic correction (Kanaya & Okayama, 1972), the maximum thickness for which the thin-film approximation is valid can be expressed as

$$\begin{aligned} t_{\max}(\text{nm}) &= 0.0495z \\ &= \frac{1.37\times10^{-5}ME_0^{5/3}}{\rho Z^{8/9}}\frac{(1+0.978\times10^{-6}E_0)^{5/3}}{(1+1.957\times10^{-6}E_0)^{4/3}} \end{aligned} \tag{29}$$

In Eq. (29), E_0 is in eV. The $t_{\max}$ values calculated from Eq. (29) for 100 and 300 keV are plotted against the atomic number in Fig. 12. The discontinuous change in the $t_{\max}$ value is due to a change in the density, similar to Fig. 2. The dashed line in Fig. 12 represents a specimen thickness of 500 nm as a marker, which might be a practical limit for X-ray analysis in conventional AEMs. Even at 100 keV, the $t_{\max}$ value is above 500 nm for most of the elements. This plot suggests that most specimens routinely used in conventional AEMs are thin enough such that Eqs (2) or (5) are valid. Therefore, the ζ-

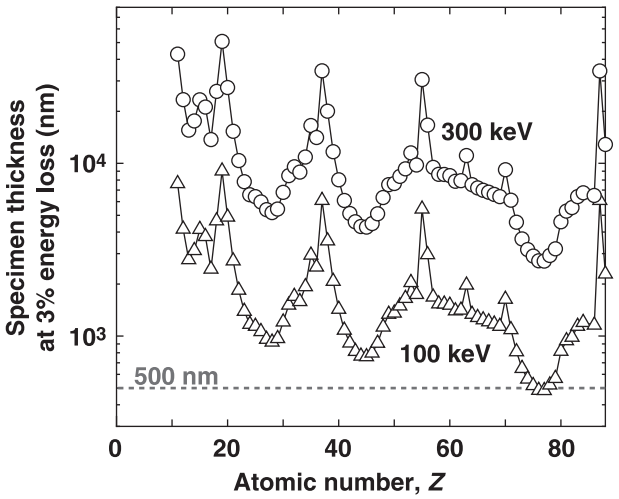

Fig. 12. A plot of the maximum applicable thickness for the pure element thin films in 100- and 300-keV instruments. The maximum applicable thickness is defined as the specimen thickness at the electron energy-loss below 3%. The dashed line represents a thickness of 500 nm. The maximum applicable thickness is higher than 500 nm in most conditions for analytical electron microscopes.

factor method is applicable for almost all thin specimens in AEMs operated at ≥ 100 keV.

Usability of PE thin-film standards. The use of PE thin-films as standards and in subsequent quantification is a major advantage and was demonstrated in Fig. 3. Obviously, the availability of PE standards overcomes many problems associated with preparation of multielement standards for *k*-factor determination. As mentioned above, several modern thin-film fabrication techniques (which can control a film thickness to within a few Ångstroms) and several approaches for accurate film-thickness measurements are available. However, a major problem with PE thin-film standards may arise from contamination and/or oxidation on the surface. Such surface contamination and oxidation can occur when the films are exposed to air after fabrication in high-vacuum equipment. Additionally, those surface contamination and oxide layers may build up during storage, prior to insertion in the AEM. In fact, most metals have native oxide layers on their surface. For example, pure Al and pure Ti natively have ~4- and 2–6-nm-thick oxide layers, respectively (e.g. Lausmaa *et al.*, 1990; Newbury, 2002). The existence of the surface layers may degrade the ζ-factor determinations and consequent quantification. One possible impact of the surface layers could be extra absorption of generated X-rays and the inadvertent ignoring of this extra absorption in the final quantification. To determine if this is a problem, X-ray absorption in the contamination and oxide layers was estimated from Eq. (8). The critical surface-layer thicknesses of the contamination (Fig. 13a) and the oxide (Fig. 13b), which would cause 5% of X-ray absorption, are plotted against the atomic number in Fig. 13. It was assumed

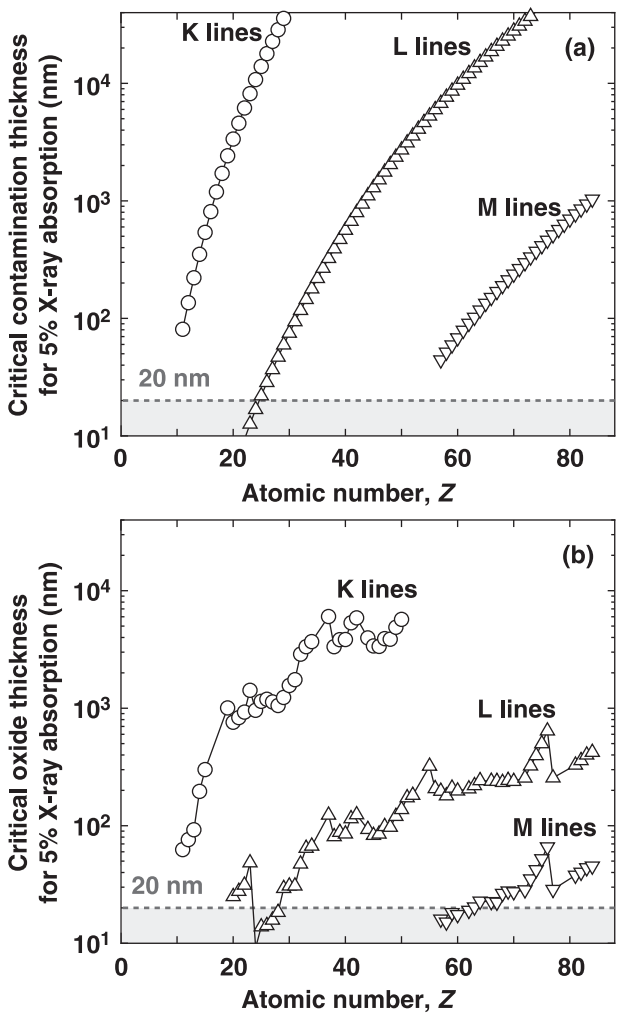

Fig. 13. The critical layer thicknesses of contamination (a) and oxide (b) on the pure element (PE) thin-film standards, which cause 5% of X-ray absorption. The shadowed area indicates the layer thickness range below 20 nm, which can be sufficient for the brief contamination or the native oxide layer on the PE thin films.

that the contamination consists of 100% carbon for the critical-thickness estimation in Fig. 13(a). It was also assumed that only one oxide type (the primary oxide) forms on the surface, as shown in Fig. 13(b). It should also be noted that information about the primary oxide (such as Al_2O_3 for Al and SnO_2 for Sn) and its density was obtained from WebElements™ (Winter, 1993). The shadowed area represents the range < 20 nm, which is estimated to be a reasonable upper boundary to the thickness of a carbon contamination layer, or the native oxide layer, on a PE film. In the case of carbon contamination, the critical layer thickness for almost all X-ray lines is > 20 nm, except for lower energy L lines from elements below Mn. As mentioned in the previous section, these lower-energy L lines are not generally used for analysis as the more reliable K lines are available. The critical oxide-layer thickness is also > 20 nm for the major X-ray lines, again with an exception for lower

energy L and M lines. Again, the elements that generate lower-energy L or M lines always generate reliable higher-energy K or L lines, respectively. Consequently, X-ray absorption due to the contamination layer or the native oxide layer on the PE thin-film standards is not crucial for the ζ-factor determination. However, if thicknesses of the PE thin films are determined with such contamination and/or oxide layers present, the ζ-factor value can be overestimated. Therefore, the thickness determination of the PE thin films must be performed as soon as the films are fabricated and re-checked if they are used after significant storage.

Beam-current measurement. The major disadvantage of the ζ-factor method is the requirement for beam-current measurement as mentioned above. Unfortunately, despite the fact that beam-current measurement is standard on almost all scanning electron microscopes (SEMs) and every EPMA, AEMs rarely come equipped with this capability, emphasizing the point that AEMs are really modified transmission electron microscopes (TEMs) and X-ray analysis is still somewhat of an afterthought. For AEMs that have no capability for direct beam-current measurements, such as the Faraday cup or the drift tube in EELS, the ζ-factor quantification is not usable. If the beam current fluctuates significantly, it may be difficult to apply the ζ-factor method. In addition, even with the beam-current measurement systems, read-out values may be inaccurate, as pointed out by Boon (2000). The systematic errors in the beam-current measurements can directly influence the mass-thickness determination and hence the subsequent absorption correction. Therefore, the beam-current measurement systems have to be checked and calibrated before applying the ζ-factor method.

Fortunately, as long as modern AEMs equipped with a Schottky field-emission gum (FEG) source are used, the beam-current fluctuation over typical time periods for analysis or mapping should be less than a few percent. The stable beam-current in Schottky FEG instruments means that the beam current does not need to be monitored frequently and can be calibrated easily through the read-out from the viewing screen. Therefore, the ζ-factor method is the ideal quantitative analysis procedure for modern instruments. Conversely, the beam current decreases with time in cold-FEG AEMs. This beam-current drop can be a serious problem for the ζ-factor quantification especially if a series of acquisitions such as line-profiling or mapping is being conducted. In this case, the effect of the beam-current drop must be corrected. Figure 14 shows the time dependence of the emission and the beam currents measured after tip-flashing in the cold-FEG VG HB 603. Whereas the emission current decreases almost linearly, the beam current drops parabolically up to 3 h after the flashing. Ideally, the beam current should be measured concurrently with a series of XEDS acquisitions. If this is not possible, however, the beam current can at least be estimated by fitting from pre- and postanalysis beam current measurements. This beam-current correction was applied to the X-ray

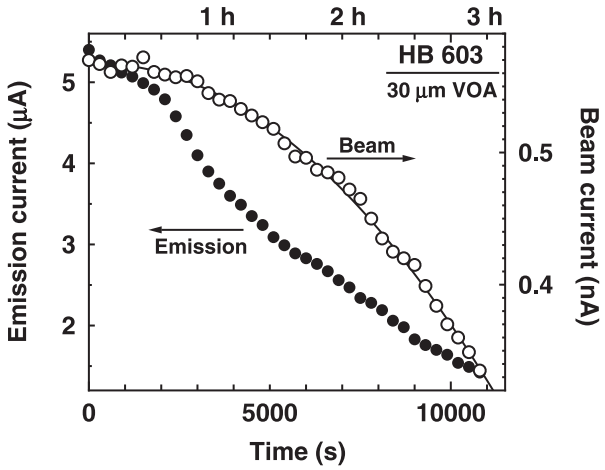

Fig. 14. Time dependence of the emission and the beam currents of cold FEG in the 300-keV VG HB 603 analytical electron microscope with a 30 μm virtual objective aperture (VOA). Both the currents were measured after flashing of the FEG tip.

maps shown in Fig. 8. In thermionic source AEMs, the beam current also decreases after stabilization. In this case, similar corrections for the beam-current drop should also be applied.

Crystalline orientation (channeling) effect. X-ray emission is influenced by the orientation of the incident beam in crystalline thin specimens (Bullock *et al.*, 1985). The orientation dependence of X-ray emission can be significant when the specimen is at specific orientations such that the reflected beams are strongly excited, e.g. in the high-symmetry zone axis and in strong Bragg diffraction conditions. This abnormal X-ray emission is useful for determination of site occupancy of impurity elements in ordered compounds, through the atom localization by channeling-enhanced microanalysis technique (e.g. Spence & Taftø, 1983). However, quantitative X-ray analysis may be compromised by such abnormal X-ray emission. In the ζ-factor method any abnormal X-ray emission results in overestimation of the specimen thickness and hence the absorption correction for soft X-rays. Therefore, it is generally recommended to avoid quantitative X-ray analysis from regions showing strong diffraction conditions. Abnormal X-ray emission can be theoretically estimated with information about the crystallographic structures and known diffraction conditions (Allen *et al.*, 1994; Rossouw *et al.*, 1997). Therefore, it is possible to incorporate 'the channeling correction term, *C*' into Eq. (9) in addition to the absorption and fluorescence corrections. The channeling correction can be challenging but it may be required for atomic-column X-ray analysis in spherical-aberration-corrected AEMs in the near future.

Ideal universal standards for L lines

Use of universal, standard, thin films is very convenient for the ζ-factor estimation. Currently, the NIST SRM 2063/2063a is

the only such standard thin film available for this purpose. As demonstrated, the SRM 2063/2063a is only applicable for K X-ray lines. However, the ζ-factors for L X-ray lines could be estimated similarly if new universal standard thin films were to become available. It would be useful to have a film containing several heavier elements, e.g. a Ge-based glass thin film (for Ge: Lα, 1.2 keV; Kα, 9.9 keV) with Mo (Lα, 2.3 keV; Kα, 17.5 keV), Ce (Mα, 0.9 keV; Lα, 4.8 keV) and W (Mα, 1.8 keV; Lα, 8.4 keV). If the ζ-factors for both K and L lines are easily determined, in addition to the use of PE thin films, then most quantitative X-ray analyses can easily be performed via this method.

The Cliff-Lorimer ratio method is > 30 years old and, whereas it is simple in concept, the need for a *k*-factor, combined with the difficulties of finding the right standard specimen, or calculating an accurate enough *k*-factor to solve a specific problem are significant limitations. The ζ-factor method overcomes the problem of standard thin specimens by the use of PE thin films or the NIST 2063/2063a standard thin specimen but requires *in-situ* measurement of the electron-beam current hitting the specimen. This disadvantage for analysis in AEMs may be overcome by the use of Schottky FEG instruments. As the electron emission from the Schottky source is very stable over the long periods of time necessary for analysis or mapping, the beam current does not need to be monitored frequently and can be calibrated easily through the read-out from the viewing screen as long as Schottky FEG-AEMs are used. Therefore, the ζ-factor method is the ideal quantitative analysis procedure for modern instruments. Once the ζ-factor method is applicable, quantitative X-ray analysis in AEMs has many advantages over the conventional Cliff-Lorimer ratio method. First, the composition can be performed with simultaneous thickness determination from the built-in absorption correction and therefore light-element materials such as ceramics can more easily be quantified in AEMs. Second, the composition and thickness data at individual analysis points can be converted routinely to give advanced levels of information, e.g. the beam broadening and spatial resolution, number of atoms in the analysed volume, and the analytical sensitivities in terms of the MMF and the MDM. Third, not only the XEDS detector efficiency but also information on the AEM–XEDS interface system can be obtained by the estimation of a series of ζ-factors, in combination with the NIST SRM 2063/2063a thin films. Therefore, the ζ-factor method may promote quantitative X-ray analysis to the next level, getting beyond the limitations of the decades-old ratio approach that, although simple in concept, has probably limited the widespread use of quantitative XEDS in thin specimens.

Acknowledgements

The authors wish to acknowledge the support of the National Science Foundation through grant DMR-0304738 and of Bechtel Bettis, Inc. They also wish to thank the reviewers in general and Dr Peter Statham in particular for their constructive comments on this paper.

References

Alber, U., Müllejans, H. & Rühle, M. (1997) Improved quantification of grain boundary segregation by EDS. *Ultramicrosc.* **69**, 105–116.

Allen, L.J., Josefsson, T.W. & Rossouw, C.J. (1994) Interaction delocalization in characteristic X-ray emission from light elements. *Ultramicrosc.* **55**, 258–267.

Armigliato, A. (1992) X-ray microanalysis in the analytical electron microscopy. *Electron Microscopy in Materials Science* (ed. by P. G. Merli and M. V. Antisari), pp. 431–456. World Scientific, Singapore.

Bambynek, W. (1984) A new evaluation of K-shell fluorescence yields. *X-84 Proceedings of the X-Ray and Inner-Shell Processes in Atoms, Molecules and Solids* (ed. by A. Meisel), post-deadline paper P-1, pp. 20–23. Leipzig.

Banchet, V., Michel, J., Jallot, E., Laurent-Maquin, D. & Balossier, G. (2003) Light elements quantitative X-ray microanalysis of thin samples in STEM. Absorption correction using EELS data. *J. Phys. D: Appl. Phys.* **36**, 1599–1604.

Bennett, J.C. & Egerton, R.F. (1995) NiO test specimens for analytical electron microscopy: round-robin results. *J. Microsc. Soc. Am.* **1**, 143–149.

Boon, G. (2000) *Simultaneous determination of specimen composition and thickness using the transmission electron microscope. PhD Dissertation*, Technische Universiteit Eindhoven.

Boon, G. & Bastin, G. (2004) Quantitative analysis of thin specimens in the TEM using a φ(ρz) -model. *Microchim. Acta*, **147**, 125–133.

Brown, D.B. (1974) Cross sections for ionization of K- and L-shells by electrons. *Handbook of Spectroscopy* (ed. by J. W. Robinson), Vol. 1, p. 248. CRC Press, Cleveland, OH.

Brown, J.M., Lortto, M.H. & Fraser, H.L. (1981) Quantitative energy-dispersive X-ray analysis of thin foils with pure elemental standards. *Analytical Electron Microscopy – 1981* (ed. by R. H. Geiss), pp. 61–64. San Francisco Press, San Francisco, CA.

Bullock, J.F., Humphreys, C.J., Mace, A.J.W., Bishop, H.E. & Titchmarsh, J.M. (1985) Crystalline effects in the analysis of semiconductor materials using Auger electrons and X-rays. *Microscopy in Semiconductor Materials 1985* (ed. by A. G. Gullis and D. B. Holt), pp. 405–410. Adam Hilger, Bristol.

Casnati, E., Tartari, A. & Baraldi, C. (1982) An empirical approach to K-shell ionization cross section by electrons. *J. Phys. B*, **15**, 155–167.

Cliff, G. & Lorimer, G.W. (1975) The quantitative analysis of thin specimens. *J. Microsc.* **103**, 203–207.

Deutsch, H., Margreiter, D. & Märk, T.D. (1994) A semi-empirical approach to the calculation of absolute inner-shell electron impact ionization cross sections. *Z. Phys. D*, **29**, 31–37.

Doig, P. & Flewitt, P.E.J. (1982) The detection of monolayer grain boundary segregation in steels using STEM-EDS X-ray microanalysis. *Met. Trans. A*, **13**, 1397–1403.

Doig, P., Lonsdale, D. & Flewitt, P.E.J. (1980) The spatial resolution of X-ray microanalysis in the scanning transmission electron microscope. *Philos. Mag. A*, **41**, 761–775.

Drawin, H.-W. (1961) Zur formelmäßigen darstellung der Ionisierungsquerschnitte gegenüber elektronenstoß. *Z. Physik*, **164**, 513–521.

Egerton, R.F. (1986) *Electron Energy-Loss Spectroscopy in the Electron Microscope*, pp. 357–359. Plenum, New York, NY.

Egerton, R.F. (1996) *Electron Energy-Loss Spectroscopy in the Electron Microscope*, 2nd edn, pp. 420–423. Plenum, New York, NY.

Egeton, R.F. & Cheng, S.C. (1994) Characterization of an analytical electron microscope with a NiO test specimen. *Ultramicrosc.* **55**, 43–54.

Eibl, O. (1993) New method for absorption correction in high-accuracy, quantitative EDX microanalysis in the TEM including low-energy X-ray lines. *Ultramicrosc.* **50**, 179–188.

Fabre de la Ripelle, M. (1949) Étude sur les coefficients spécifiques d'ionisation. *J. Phys. Radium*, **10**, 319–329.

Fiori, C.E., Swyt, C.R. & Myklebust, R.L. (1992) *NIST/NIH Desk Top Spectrum Analyzer*, available from the National Institute of Standards and Technology, Gaithersburg, MD (http://www.cstl.nist.gov/div837/Division/outputs/DTSA/DTSA.htm).

Foitzik, A.H., Sears, J.S., Xiao, S.-Q., Heuer, A.H. & Wunderlich, W. (1993) On a high-purity Ge EDS detector II. Ice layer formation and optimization of detector design. *Ultramicrosc.* **50**, 219–227.

Galassi, M., Davies, J., Theiler, J., Gough, B., Jungman, G., Booth, M. & Rossi, F. (2002) *Gnu Scientific Library: Reference Manual*, 2nd edn. Network Theory Ltd, Bristol (information also available at http://www.gnu.org/software/gsl/manual/gsl-ref_toc.html).

Goldstein, J.I., Costley, J.L., Lorimer, G.W. & Reed, R.J.B. (1977) Quantitative X-ray analysis in the electron microscope. *Scanning Electron Microscopy – 1977* (ed. by O. Johari), Vol. 1, pp. 315–324. IITRI, Chicago, IL.

Gorzkowski, E.P., Watanabe, M., Scotch, A.M., Chan, H.M. & Harmer, M.P. (2004) Direct measurement of oxygen in lead-based ceramics using the ζ-factor method in an analytical electron microscope. *J. Mater. Sci.* **39**, 6735–6741.

Green, M. & Cosslett, V.E. (1961) The efficiency of production of characteristic X-radiation in thick targets of a pure element. *Proc. Phys. Soc.* **78**, 1206–1214.

Gryzinski, M. (1965) Classical theory of atomic collisions. I. Theory of inelastic collisions. *Phys. Rev.* **138**, 336–358.

Heinrich, K.F.J. (1987) Mass absorption coefficients for electron probe microanalysis. *Proceedings of the 11th International Congress on X-Ray Optics and Microanalysis* (ed. by J. D. Brown and R. H. Packwod), pp. 67–377. University of Western Ontario, London, Ontario.

Horita, Z., Sano, T. & Nemoto, M. (1987) Simplification of X-ray absorption correction in thin-sample quantitative microanalysis. *Ultramicrosc.* **21**, 271–276.

Horita, Z., Ichitani, K., Sano, T. & Nemoto, M. (1989) Application of the differential X-ray absorption method to the determinations of foil thickness and local composition in the analytical electron microscope. *Phil. Mag. A*, **59**, 939–952.

Jakoby, C., Genz, H. & Richter, A. (1987) A semi-empirical formula for the total K-shell ionization cross section by electron impact. *J. de Physiq. Colloq.*, **C9**, 487–490.

Joy, D.C. & Maher, D.M. (1977) Sensitivity limits for thin specimen X-ray analysis. *Scanning Electron Microscopy – 1977* (ed. by O. Johari), Vol. 1, pp. 325–334. IITRI, Chicago, IL.

Kanaya, K. & Okayama, S. (1972) Penetration and energy-loss theory of electrons in solid targets. *J. Phys. D*, **5**, 43–58.

Keast, V.J. & Williams, D.B. (2000) Quantification of boundary segregation in the analytical electron microscope. *J. Microsc.* **199**, 45–55.

King, W.E. (1985) An experimental technique to measure X-ray production and detection efficiencies in the analytical electron microscope. *Ultramicrosc.* **18**, 151–154.

Kolbenstvedt, H. (1967) Simple theory for K-ionization by relativistic electrons. *J. Appl. Phys.* **38**, 4785–4787.

Kreyszig, E. (1999) *Advanced Engineering Mathematics*, 8th edn, pp. 1109–1116. John Wiley & Sons, New York, NY.

Lausmaa, J., Kasemo, B. & Mattsson, H. (1990) Surface spectroscopic characterization of titanium implant materials. *Appl. Surf. Sci.* **44**, 133–146.

Liebhafsky, H.A., Pfeiffer, H.G. & Zemany, P.D. (1955) Precision in X-ray emission spectrography. *Anal. Chem.* **27**, 1257–1258.

Lotz, W. (1967) An empirical formula for the electron-impact ionization cross-section. *Z. Physik*, **206**, 205–211.

Lyman, C.E., Goldstein, J.I., Williams, D.B., Ackland, D.W., von Harrach, H.S., Nicholls, A.W. & Statham, P.J. (1994) High performance X-ray detection in a new analytical electron microscopy. *J. Microsc.* **176**, 85–98.

Lyons, L. (1991) *A Practical Guide to Data Analysis for Physical Science Students*. Cambridge University Press, Cambridge.

Maher, D.M., Joy, D.C., Ellington, M.B., Zaluzec, N.J. & Mochel, P.E. (1981) Relative accuracy of k-factor calculations for thin-film X-ray analysis. *Analytical Electron Microscopy – 1981* (ed. by R. H. Geiss), pp. 33–38. San Francisco Press, San Francisco, CA.

Michael, J.R. (1987) *Practical Analytical Electron Microscopy in Materials Science*, 2nd edn (ed. by D. B. Williams), pp. 82–83. Philips Electron Optics Publishing Group, Mahwah, NJ.

Michael, J.R. (1995) Energy dispersive X-ray spectrometry in ultra-high vacuum environments. *X-Ray Spectrometry in Electron Beam Instruments* (ed. by D. B. Williams, J. I. Gildstein and D. E. Newbury), pp. 83–99. Plenum, New York, NY.

Michael, J.R., Williams, D.B., Klein, C.F. & Ayer, R. (1990) The measurement and calculation of the X-ray spatial resolution obtained in the analytical electron microscope. *J. Microsc.* **160**, 41–53.

Morris, P.L., Ball, M.D. & Statham, P.J. (1980) The correction of thin foil microanalysis data for X-ray absorption effect. *Developments in Electron Microscopy and Analysis* (ed. by T. Mulvey), pp. 413–416. The Institute of Physics, London.

Mott, N.F. & Massey, H.S.W. (1949) *The Theory of Atomic Collisions*. Clarendon Press, Oxford.

Newbury, D.E. (2002) Barriers to quantitative electron probe X-ray microanalysis for low voltage scanning electron microscopy. *J. Res. Natl Inst. Stand. Technol.* **107**, 605–619.

Newbury, D.E., Williams, D.B., Goldstein, J.I. & Fiori, C.E. (1984) Observation on the calculation of k_{AB} factors for analytical electron microscopy. *Analytical Electron Microscopy – 1984* (ed. by D. B. Williams and D. C. Joy), pp. 276–278. San Francisco Press, San Francisco, CA.

Nockolds, C., Nasir, M.J., Cliff, G. & Lorimer, G.W. (1980) X-ray fluorescence correction in thin foil analysis and direct methods for thickness measurement. *Developments in Electron Microscopy and Analysis* (ed. by T. Mulvey), pp. 417–420. The Institute of Physics, London.

Ogilvie, R.E. (1984) K-shell ionization cross sections employing a modified Arthurs and Moiseiwitsch equation. *Analytical Electron Microscopy – 1984* (ed. by D. B. Williams and D. C. Joy), pp. 299–302. San Francisco Press, San Francisco, CA.

Okamoto, K., Ohkura, Y., Naruse, M., Hasegawa, K., Deguchi, S., Kawazoe, M. & Kersker, M. (2003) A newly developed PC controlled 200kV FE-TEM. *Microsc. Microanal.* 9 (Suppl. 2) (ed. by D. Piston, J. Bruley, I. M. Anderson, P. Kotula, G. Solorzano, A. Lockley and S. McKernan), pp. 1272CD–1273CD. Cambridge University Press, New York.

Paterson, J.H., Chapman, J.N., Nicholson, W.A.P. & Titchmarsh, J.M. (1989) Characteristic X-ray production cross-sections for standardless elemental analysis in EDX. *J. Microsc.* **154**, 1–17.

Philibert, J. (1963) A method for calculating the absorption correction in electron-probe microanalysis. *Proceedings of the 3rd International Congress on X-Ray Optics and Microanalysis* (ed. by H. H. Pattee, V. E. Cosslett and A. Engström), pp. 379–392. Academic Press, New York, NY.

Philibert, J. & Tixier, R. (1975) Electron probe microanalysis of transmission electron microscope specimens. *Physical Aspects of Electron Microscopy and Microbeam Analysis* (ed. by B. M. Siegel and D. R. Beaman), pp. 333–354. John Wiley & Sons, New York, NY.

Philibert, J., Rivory, J., Bryckaert, D. & Tixier, R. (1970) Electron probe microanalysis on electron microscope thin foils using thin standards. *J. Phys. D*, **3**, L70–L72.

Porter, D.A. & Westengen, H. (1981) STEM microanalysis of intermetallic phases in an Al-Fe-Si alloy. *Quantitative Microanalysis with High Spatial Resolution* (ed. by G. W. Lorimer, M. H. Jacobs and P. Doig), pp. 94–100. The Metals Society, London.

Pouchou, J.L. (1994) Standardless X-ray analysis of bulk specimens. *Mikrochim. Acta*, **114/115**, 33–52.

Pouchou, J.L. & Pichoir, F. (1991) Quantitative analysis of homogeneous or stratified microvolumes applying the model 'PAP'. *Electron Probe Quantification* (ed. by K. F. J. Heinrich and D. E. Newbury), pp. 31–75. Plenum, New York, NY.

Powell, C.J. (1976a) Evaluation of formulas for inner-shell ionization cross sections. *Proceedings of the Use of Monte Carlo Calculations in Electron Probe Microanalysis and Scanning Electron Microscopy* (ed. by K. F. J. Heinrich, D. E. Newbury and H. Yakowitz), pp. 97–104. National Bureau of Standards Special Publication 460, Gaithersburg, MD.

Powell, C.J. (1976b) Cross sections for ionization of inner-shell electrons by electrons. *Rev. Mod. Phys.* **48**, 33–47.

Press, W.H., Teukolsky, S.A., Vetterling, W.T. & Flannery, B.P. (2002) *Numerical Recipes in C++: the Art of Scientific Computing*, 2nd edn. Cambridge University Press, Cambridge.

Quarles, C.A. (1976) Semiempirical analysis of electron-induced K-shell ionization. *Phys. Rev. A*, **13**, 1278–1280.

Rasberry, S.D. (1987) *Certificate of Analysis for Standard Reference Material 206 3.* National Bureau of Standards (now National Institute of Standards and Technology), Gaithersburg, MD.

Reed, S.J.B. (1982) The single scattering model and spatial resolution in X-ray analysis of thin foils. *Ultramicrosc.* **7**, 405–409.

Reed, W.P. (1993a) *Certificate of Analysis for Standard Reference Material 206 3a.* National Institute of Standards and Technology, Gaithersburg, MD.

Reed, S.J.B. (1993b) *Electron Microprobe Analysis*, 2nd edn, pp. 197–198. Cambridge University Press, Cambridge.

Romig, A.D. Jr & Goldstein, J.I. (1979) Detectability limit and spatial resolution in STEM X-ray analysis: application to Fe-Ni. *Microbeam Analysis – 1979* (ed. by D. E. Newbury), pp. 124–128. San Francisco Press, San Francisco, CA.

Rossouw, C.J., Forwood, C.T., Gibson, M.A. & Miller, P.R. (1997) Generation and absorption of characteristic X-rays under dynamical electron diffraction conditions. *Micron*, **28**, 125–137.

Schreiber, T.P. & Wims, A.W. (1981) A quantitative X-ray microanalysis thin film method using K-, L-, and M-lines. *Ultramicrosc.* **6**, 323–334.

Sheridan, P.H. (1989) Determination of experimental and theoretical k_{ASi} factors for a 200 kV analytical electron microscope. *J. Electr. Microsc. Techn.* **11**, 41–61.

Spence, J.C.H. & Taftø, J. (1983) ALCHEMI: a new technique for locating atoms in small crystals. *J. Microsc.* **130**, 147–154.

Statham, P.J. (1998) Recent developments in instrumentation for X-ray microanalysis. *Mikrochim. Acta Suppl.* **15**, 1–9.

Statham, P.J. & Ball, M.D. (1980) An indirect method for determining mass thickness for absorption corrections in the microanalysis of thin foils. *Microbeam Analysis – 1980* (ed. by D. B. Wittry), pp. 165–168. San Francisco Press, San Francisco, CA.

Steel, E.B., Newbury, D.E. & Pella, P.A. (1981) Preparation of thin-film glass standards for analytical electon microscopy. *Analytical Electron Microscopy – 1981* (ed. by R. H. Geiss), pp. 65–70. San Francisco Press, San Francisco, CA.

Steel, E.B., Marinenko, R.B. & Myklebust, R.L. (1997) Quality assurance of energy dispersive spectrometry systems. *Microsc. Microanal.* **3** (Suppl. 2) (ed. by G. W. Bailey, R. V. W. Dimlich, K. B. Alexander, J. J. McCarthy and T. P. Pretlow), pp. 903–904. Springer, New York.

Thomas, B., Chemelle, P. & Bourgeot, J. (1984) Quantitative analytical electron microscopy with use of bulk standards. *Analytical Electron Microscopy – 1984* (ed. by D. B. Williams and D. C. Joy), pp. 311–314. San Francisco Press, San Francisco, CA.

Thompson, W.J. (2001) Poisson distributions. *Comp. Sci. Eng.* 3, May/June issue, 78–82.

Van Cappellen, E. (1990) The parameterless correction method in X-ray microanalysis. *Microsc. Microanal. Microstruct.* **1**, 1–22.

Van Cappellen, E. & Schmitz, A. (1992) A simple spot-size versus pixel-size criterion for X-ray microanalysis of thin foils. *Ultramicrosc.* **41**, 193–199.

Watanabe, M. & Williams, D.B. (1999a) The new form of the ζ-factor method for quantitative microanalysis in AEM-XEDS and its evaluation. *Microsc. Microanal.* 5 (Suppl. 2) (ed. by G. W. Bailey, W. G. Jerome, S. McKernan, J. F. Mansfield and R. L. Price), pp. 88–89. Springer, New York.

Watanabe, M. & Williams, D.B. (1999b) Atomic-level detection by X-ray microanalysis in the analytical electron microscope. *Ultramicrosc.* **78**, 89–101.

Watanabe, M. & Williams, D.B. (2003) Quantification of elemental segregation to lath and grain boundaries in low-alloy steel by STEM X-ray mapping combined with the ζ-factor method. *Z. Metallk.* **94**, 307–316.

Watanabe, M., Horita, Z. & Nemoto, M. (1996) Absorption correction and thickness determination using ζ-factor in quantitative X-ray microanalysis. *Ultramicrosc.* **65**, 187–198.

Williams, D.B. & Carter, C.B. (1996) *Transmission Electron Microscopy: a Textbook for Materials Science*. Plenum, New York, NY.

Williams, D.B., Michael, J.R., Goldstein, J.I. & Romig, A.D. Jr (1992) Definition of the spatial resolution in X-ray microanalysis in thin foils. *Ultramicrosc.* **47**, 121–132.

Williams, D.B., Watanabe, M. & Carpenter, D.T. (1998) Thin film analysis and chemical mapping in the analytical electron microscope. *Mikrochim. Acta Suppl.* **15**, 49–57.

Williams, D.B., Papworth, A.J. & Watanabe, M. (2002) High resolution X-ray mapping in the STEM. *J. Electr. Microsc.* **51S**, S113–S126.

Winter, M.J. (1993) *WebElements™*. Available at http://www.webelements.com.

Wood, J.E., Williams, D.B. & Goldstein, J.I. (1984) Experimental and theoretical determination of k_{AFe} factors for quantitative X-ray microanalysis in the analytical electron microscope. *J. Microsc.* **133**, 255–274.

Worthington, C.R. & Tomlin, S.G. (1956) The intensity of emission of characteristic X-radiation. *Proc. Phys. Soc. Lond. A*, **69**, 401–412.

Zaluzec, N.J. (1984) K- and L-cross sections for X-ray microanalysis in an AEM. *Analytical Electron Microscopy – 1984* (ed. by D. B. Williams and D. C. Joy), pp. 279–284. San Francisco Press, San Francisco, CA.

Zemyan, S.M. (1995) *The formation and characterization of metal alloy aerosols. PhD Dissertation*, Lehigh University.